Available online at www.sciencedirect.com

ScienceDirect

Geochimica et Cosmochimica Acta 71 (2007) 5117–5134

Geochimica et Cosmochimica Acta

www.elsevier.com/locate/gca

Calcium isotope record of Phanerozoic oceans: Implications for chemical evolution of seawater and its causative mechanisms

Juraj Farkaš [a,*,1], Florian Böhm [b], Klaus Wallmann [b], John Blenkinsop [c], Anton Eisenhauer [b], Robert van Geldern [d], Axel Munnecke [e], Silke Voigt [b], Ján Veizer [a]

[a] *University of Ottawa and Ottawa–Carleton Geoscience Centre, Ottawa, Ont., Canada K1N 6N5*
[b] *Leibniz Institute of Marine Sciences, IFM-GEOMAR, D-24148 Kiel, Germany*
[c] *Carleton University and Ottawa–Carleton Geoscience Centre, Ottawa, Ont., Canada K1S 5B6*
[d] *Leibniz Institute for Applied Geosciences, Stilleweg 2, 30655 Hannover, Germany*
[e] *Palaeontological Institute of the Friedrich-Alexander University, D-91054 Erlangen, Germany*

Received 6 June 2007; accepted in revised form 10 September 2007; available online 22 September 2007

Abstract

A total of 280 brachiopods of Ordovician to Cretaceous age, complemented by published data from belemnites and planktonic foraminifera, are used to reconstruct the evolution of calcium isotope composition of seawater ($\delta^{44/40}Ca_{SW}$) over the Phanerozoic. The compiled $\delta^{44/40}Ca_{SW}$ record shows a general increase from ~1.3‰ (NIST SRM 915a) at the beginning of the Ordovician to ~2‰ at present. Superimposed on this trend is a major long-term positive excursion from the Early Carboniferous to Early Permian as well as several short-term, mostly negative, oscillations.

A numerical model of the global cycles of calcium, carbon, magnesium and strontium was used to estimate whether the recorded $\delta^{44/40}Ca_{SW}$ variations can be explained by varying magnitudes of input and output fluxes of calcium to the oceans. The model uses the record of marine $^{87}Sr/^{86}Sr$ ratios as proxy for seafloor spreading rates, a record of oceanic Mg/Ca ratios to estimate rates of dolomite formation, and reconstructed atmospheric CO_2, discharge and erosion rates to estimate continental weathering fluxes.

The model results indicate that varying magnitudes of the calcium input and output fluxes cannot explain the observed $\delta^{44/40}Ca_{SW}$ trends, suggesting that the isotope signatures of these fluxes must also have changed. As a possible mechanism we suggest variable isotope fractionation in the sedimentary output flux controlled by the dominant mineralogy in marine carbonate deposits, i.e. the oscillating 'calcite–aragonite seas'. The ultimate control of the calcium isotope budget of the Phanerozoic oceans appears to have been tectonic processes, specifically variable rates of oceanic crust production that modulated the hydrothermal calcium flux and the oceanic Mg/Ca ratio, which in turn controlled the dominant mineralogy of marine carbonates, hence the $\delta^{44/40}Ca_{SW}$. As to the causes of the short-term oscillations recorded in the secular $\delta^{44/40}Ca_{SW}$ trend, we tentatively propose that these are related to variable rates of dolomite formation and/or to changing chemical composition of the riverine flux, in particular Ca/HCO_3^- and Ca/SO_4^{2-} ratios, induced by variable proportions of silicate vs. carbonate weathering rates on the continents.

---

[*] Corresponding author. Fax: +1 617 495 8839.
E-mail address: jfarkas@eps.harvard.edu (J. Farkaš).

[1] Present address: Department of Earth and Planetary Sciences, Harvard University, 20 Oxford Street, Cambridge, MA 02138-2902, USA.

0016-7037/$ - see front matter © 2007 Elsevier Ltd. All rights reserved.
doi:10.1016/j.gca.2007.09.004

1. INTRODUCTION

One of the primary research interests of earth system sciences is to constrain the chemical and isotope evolution of the oceans over geological time, as processes that control seawater chemistry also affect the composition of the atmosphere that, in turn, modulates the Earth's climate. The major ion and isotope composition of seawater varied significantly over the Phanerozoic, as suggested by the fluid inclusion data of primary marine halite (Lowenstein et al., 2001, 2003; Horita et al., 2002), by the elemental and isotope compositions of marine skeletal carbonates (Veizer et al., 1999; Dickson, 2002; Steuber and Veizer, 2002; Kampschulte and Strauss, 2004), and by changing mineralogy of marine carbonates and potash evaporites (Sandberg, 1983; Hardie, 1996). The synchronous nature of these temporal trends indicates that they may have been controlled by a common causative mechanism (Horita et al., 2002), but as yet there is no consensus as to the identity of this underlying mechanism (Veizer and Mackenzie, 2003; Holland, 2005).

Two main contenders have been advocated as principal drivers of chemical and isotope evolution of seawater during the Phanerozoic. One group of explanations (Spencer and Hardie, 1990; Hardie, 1996; Steuber and Veizer, 2002) regards plate tectonics as the ultimate driving force. In this alternative, ocean chemistry varied mostly due to variable seawater cycling rates via submarine hydrothermal systems, which in turn are controlled by seafloor spreading rates and by the total volume of mid-ocean ridges. An alternative, or complementary, hypothesis (Holland and Zimmermann, 2000; Zimmermann, 2000; Berner, 2004; Holland, 2005) argues that seawater chemistry was largely controlled by sedimentological factors, such as variable rates of dolomite and/or gypsum (anhydrite) deposition, with a possible although relatively minor contribution from the submarine hydrothermal systems.

The relative importance of these causative factors can potentially be resolved by novel analytical techniques, such as the isotope systems of calcium and magnesium. The calcium isotope record, based on marine skeletal carbonates, has already proved to be a useful indicator of changing intensity of oceanic calcium fluxes (Heuser et al., 2005), particularly of their hydrothermal component (Farkaš et al., 2007).

In this study, we reconstruct the calcium isotope evolution of seawater ($\delta^{44/40}Ca_{SW}$) during the Phanerozoic, based on brachiopods as carrier phases and supplemented by literature data from marine carbonates (Heuser et al., 2005; Steuber and Buhl, 2006; Farkaš et al., 2007) and phosphates (Schmitt et al., 2003a; Soudry et al., 2004, 2006). This empirical Phanerozoic $\delta^{44/40}Ca_{SW}$ record is subsequently simulated by an expanded version of the numerical model for coupled calcium/carbon/magnesium global cycles (Hansen and Wallmann, 2003; Wallmann, 2004; Heuser et al., 2005).

Our calcium isotope data represent the first continuous $\delta^{44/40}Ca_{SW}$ record for the Paleozoic and complemented by literature data (De La Rocha and DePaolo, 2000; Schmitt et al., 2003a; Soudry et al., 2004, 2006; Fantle and DePaolo, 2005, 2007; Heuser et al., 2005; Kasemann et al., 2005; Steuber and Buhl, 2006; Farkaš et al., 2007), this study presents the first $\delta^{44/40}Ca_{SW}$ record across the entire Phanerozoic.

2. MATERIALS AND METHODS

2.1. Materials

We analyzed calcium isotope composition of 280 brachiopod shells of Ordovician to modern ages, thus covering most of the Phanerozoic time span. The $\delta^{44/40}Ca_{SW}$ record is based for the most part (~87%) on our brachiopod samples, but the Cenozoic, Cretaceous, and Middle/Late Jurassic portions are mostly constrained by literature data ($n = 139$).

Specifically, we measured $\delta^{44/40}Ca$ values of low-Mg calcite that was sampled from the interior 'secondary' layer of brachiopod shells. This layer is fairly resistant to post-depositional alteration (Veizer et al., 1999; Samtleben et al., 2001). Most of these shells were previously analyzed for their trace element (Sr, Mn, Fe) and isotope ($^{87}Sr/^{86}Sr$, $\delta^{18}O$, $\delta^{13}C$ and $\delta^{34}S$) compositions and were also screened by cathodoluminescence (CL) and scanning electron microscopy (SEM) in order to evaluate their state of preservation (Veizer et al., 1999; Samtleben et al., 2000, 2001; Kampschulte and Strauss, 2004; Voigt et al., 2004; van Geldern et al., 2006).

The samples for the present study were selected utilizing the following textural and geochemical criteria: (i) the calcite was non-luminescent and retained its original ultrastructure; (ii) had high Sr/Mn ratio (Veizer, 1983); and (iii) the lowest $^{87}Sr/^{86}Sr$ among the coeval or stratigraphically close samples (Veizer et al., 1999). We adopted this approach because diagenetic alteration of marine carbonates tends to increase their $^{87}Sr/^{86}Sr$ ratios while decreasing Sr/Mn and induces typical yellow/orange luminescence (Veizer, 1983; Veizer et al., 1999).

Brachiopods were collected in the USA (including San Juan Island), Canada (including Anticosti Island), Great Britain, Ireland, Germany, Sweden (including Gotland), Belgium, Austria, Italy, Spain, Morocco, Lithuania, Latvia, Hungary, Ukraine, Russia, China and Australia. Further details on location, stratigraphy and the additional geochemical data are available in Veizer et al. (1999), Samtleben et al. (2000, 2001), Calner et al. (2004), Voigt et al. (2004), Jeppsson et al. (2006) and van Geldern et al. (2006). Based on the paleogeographic reconstructions of Scotese et al. (1994) and Scotese (1997) most of the samples originated from tropical to subtropical regions, representing a paleolatitudinal range from 30°N to 30°S.

The time scale used in our figures is from Harland et al. (1990) to enable correlation with the previously published datasets (Veizer et al., 1999) that were used as controlling variables for our geochemical modeling. For ease of comparison, we converted the numerical ages of Harland et al. (1990) also into the time scale of Gradstein et al. (2004), using simple linear interpolation between the stage boundaries (see Appendix, Tables EA-4 and EA-5).

2.2. Methods

2.2.1. Sample preparation and analytical methods

Powders composed of low-Mg calcite were sampled using a micro-drill then weighed into a Teflon PFA (perfluoroaloxy) vial and ultrasonically cleaned in ultrapure water (>18 MΩ cm) for about 30 min. The cleaning procedure was repeated at least twice. To remove the organic matter causing isobaric interferences during the calcium isotope analysis (Hippler et al., 2004; Böhm et al., 2006) the powders were also ultrasonically cleaned with 30% H_2O_2 at Ottawa/Carleton. A mixture of HNO_3–H_2O_2 was added to the sample solution during spike addition at IFM-GEOMAR as described in Böhm et al. (2006). These solutions were evaporated to dryness at 80 °C and dissolved in an adjusted volume of 2 N HCl. All chemicals used in this study were of high purity with sub-ppb levels of metal concentrations.

The calcium isotope measurements were performed on Thermo Electron Triton TIMS thermal ionization mass spectrometers in Ottawa, Canada (Carleton University) and in Kiel, Germany (IFM-GEOMAR). The isotope composition was determined by a conventional double spiking technique (Russell et al., 1978) using a ^{43}Ca/^{48}Ca double spike (Heuser et al., 2002). For the data reduction we used an iterative algorithm of Heuser et al. (2002) with an exponential term for the fractionation correction. This approach allowed us to calculate the original ^{44}Ca/^{40}Ca ratio of a sample from the measured ^{40}Ca/^{48}Ca, ^{43}Ca/^{48}Ca and ^{44}Ca/^{48}Ca ratios (at Ottawa–Carleton) or ^{40}Ca/^{43}Ca and ^{44}Ca/^{43}Ca ratios (at IFM-GEOMAR) in a sample/spike mixture and from the isotope composition of our ^{43}Ca/^{48}Ca double spike.

Analytical results are expressed as $\delta^{44/40}$Ca values in permil (‰) relative to the NIST SRM 915a $CaCO_3$ standard, using the following relation (Eisenhauer et al., 2004): $\delta^{44/40}\mathrm{Ca} = [(^{44}\mathrm{Ca}/^{40}\mathrm{Ca})_{\mathrm{sample}}/(^{44}\mathrm{Ca}/^{40}\mathrm{Ca})_{\mathrm{standard}} - 1] \times 1000$. The external precision for $\delta^{44/40}$Ca is expressed as two standard deviations ($\pm 2\sigma$) determined by repeat measurements from the same sample solution. The potential influence of radiogenic ^{40}Ca on measured $\delta^{44/40}$Ca was tested on selected Devonian brachiopod samples and was found to be negligible at the level of our analytical uncertainty, ±0.15‰ (for details see Section 2.2.3).

2.2.2. Ottawa/Carleton: calcium isotope experimental procedures

A total of 210 brachiopods (Ordovician, Silurian, Devonian, Carboniferous, Permian, Triassic and modern) were analyzed for their $\delta^{44/40}$Ca at Carleton University in the Isotope Geochemistry and Geochronology Research Centre (IGGRC). The analytical technique is based on the method described in Farkaš et al. (2007) with a few modifications adopted for the chemical preparation and data acquisition. Specifically, we skipped the chromatographic clean-up (see below), except for seawater, and introduced a fully automated routine for the calcium isotope analysis (see Appendix EA-1), which significantly increased the sample throughput allowing us to analyze up to 10 samples over the course of 24 h.

Experimental testing on brachiopods with variable trace element contents (Table 1) showed that chromatographic clean-up on cation-exchange columns is not necessary for relatively pure biogenic carbonates. The influence of carbonate matrix on measured $\delta^{44/40}$Ca was investigated on two aliquots of the same sample, one prepared by direct dissolution and the other passed through a cation-exchange column filled with BioRad AG50W resin (Farkaš et al., 2007). The measured $\delta^{44/40}$Ca values of these two aliquots were identical, within ±0.15‰, for all the cases (Table 1), suggesting only a negligible or no influence of carbonate matrix on measured $\delta^{44/40}$Ca.

A brief description of this modified method is presented below. Weighed samples (~1000 μg of powdered $CaCO_3$) were dissolved in 1000 μL of 2 M HCl in a PFA Teflon vial. From this solution 25 μL (~10 μg Ca) were pipetted into a new vial and mixed with 65 μL of a Ca isotope double spike solution with ^{43}Ca/^{48}Ca of 0.7221 ± 0.0004 (2σ, $n = 8$) Farkaš et al. (2007). As a result, the ^{40}Ca/^{48}Ca ratio of a mixture was approximately 60, usually somewhere between 55 and 65. After the double spiking, the mixture was evaporated to dryness and redissolved in 10 μL of 5% HNO_3. From this solution 3 μL (3 μg Ca) were loaded as a nitrate on a zone-refined Re ribbon of a double filament assembly. The sample solution was dried at a filament current of 0.5 ampere (A), heated at 1.5 A for 60 s and finally brought to dull red at about 2.2 A for 30 s.

In the mass spectrometer, the samples were heated to an ionization temperature of about 1400 °C using an automatic sequence with a built-in program for sample heating (see Appendix EA-1, Table EA-1). The target ion beam intensity for ^{40}Ca signal was 130 pA (13,000 mV) and this was usually reached within ~30 min. The sample heating sequence was followed by an automated data acquisition routine. The calcium isotope peaks (masses 40–48) were measured in two steps, including ^{41}K that was monitored for possible isobaric interferences of ^{40}K on ^{40}Ca. An individual measurement consisted of 108 cycles, 9 blocks of 12 cycles each, with an integration time of 16-s per cycle

Table 1
The effect of chromatographic clean-up on measured $\delta^{44/40}$Ca of modern (Y342L) and fossil (Devonian: D176; Silurian: G68) brachiopods

Sample	Material	Mg (wt%)	Sr (ppm)	Fe (ppm)	Direct dissolution (Ca fraction + matrix)	Chromatography[a] (Ca fraction only)
					$\delta^{44/40}$Ca (‰) (2σ)[b]	$\delta^{44/40}$Ca (‰) (2σ)[b]
Y342L	Brachiopod	0.15	1085	6	1.05 ± 0.01	1.07 ± 0.01
D176	Brachiopod	0.58	592	1954	0.73 ± 0.07	0.75 ± 0.04
G68	Brachiopod	0.20	2042	—	0.48 ± 0.03	0.54 ± 0.08

[a] Samples were passed through cation-exchange micro-columns filled with BioRad AG50W resin.

[b] External precision was determined as 2σ from two measurements of the same sample solution.

followed by a 3-s waiting time. Defocused baselines measurements were collected for 30 s at the beginning of each block. A total analytical time of this fully automated routine was about 150 min per sample (30 min for the heating plus 120 min for the data acquisition).

The external precision of $\delta^{44/40}$Ca, as determined by the repeat analysis of NIST SRM 915a over a period of 6 months, was ±0.13‰ (2σ, $n = 30$) with a mean ^{44}Ca/^{40}Ca ratio of 0.021538 ± 0.000003 (2σ), the latter value was also used as a normalizing ratio for $\delta^{44/40}$Ca. The measured $\delta^{44/40}$Ca (NIST SRM 915a) value of IAPSO seawater yielded 1.86 ± 0.20‰ (2σ, $n = 5$), in agreement with the published value of 1.88 ± 0.04‰ (Hippler et al., 2003). The total procedural Ca blank was consistently below 15 ng of the loaded 3 µg, i.e. less than 1%.

2.2.3. *IFM-GEOMAR: calcium isotope experimental procedures*

The calcium isotope analyses of 70 brachiopods (Silurian, Devonian and Cretaceous) were performed at the mass spectrometer facilities of the IFM-GEOMAR (Leibniz Institute of Marine Sciences) in Kiel, Germany, following the method described in Heuser et al. (2002) and Böhm et al. (2006).

Briefly, sample powders were dissolved in 2 N HCl, evaporated and redissolved so the concentration of calcium in a solution would be ∼0.15 µg per µL. From this solution, ∼0.3 µg of Ca was spiked with 10 µL of a ^{43}Ca/^{48}Ca double spike, evaporated to dryness, and loaded with 2 N HCl and a $TaCl_5$ activator on a single zone-refined Re filament. Sample filaments were heated to a temperature of ∼1500 °C, corresponding to a filament current of about 3 A and a ^{40}Ca signal intensity of about 40 pA (4000 mV). The heating procedure typically lasted 40 min. Data were collected in dynamic mode with ^{40}Ca, ^{42}Ca, ^{43}Ca and ^{44}Ca peaks measured in the first cycle, and ^{43}Ca, ^{44}Ca and ^{48}Ca in the second cycle. The intensity of ^{40}Ca during the measurement was 40–50 pA (4000–5000 mV). Data were acquired for about 50 min (7 blocks of 22 cycles each).

Typical external precision for $\delta^{44/40}$Ca was ±0.1‰ (2σ) and the long-term (4 years) mean for ^{44}Ca/^{40}Ca of SRM 915a is 0.021182 ± 0.000006 (2σ, $n = 289$). The $\delta^{44/40}$Ca value of IAPSO seawater, normalized to SRM 915a, showed heavy isotope enrichment of 1.89 ± 0.1‰ (2σ, $n = 20$). The long-term (2 years) mean ^{44}Ca/^{40}Ca ratio of IAPSO was measured as 0.021222 ± 0.000008 (2σ, $n = 20$). Total Ca blanks were less than 2 ng of the loaded 300 ng, i.e. less than 1%.

We observed a minor but consistent inter-laboratory bias where the $\delta^{44/40}$Ca values measured at IFM-GEOMAR are about 0.15‰ lighter compared to data acquired at Ottawa/Carleton (Fig. 1), thus all data measured at IFM-GEOMAR were adjusted by adding 0.15‰. This offset is most likely a consequence of different loading techniques used in the above laboratories (double filament and HNO_3 vs. single filament and $TaCl_5$).

For the determination of radiogenic ^{40}Ca about 1 µg of Ca was prepared and loaded on a single zone-refined Re filament as described above, however without addition of a double spike. Sample filaments were heated to about 1550 °C corresponding to a ^{40}Ca signal intensity of about 100 pA (10 V). Data for masses ^{40}Ca, ^{42}Ca and ^{44}Ca were collected in static mode. The measured ^{40}Ca/^{44}Ca ratios were corrected for mass fractionation to a ^{42}Ca/^{44}Ca value of 0.31221 (DePaolo, 2004) using an exponential fractionation law. Data were acquired for up to 75 min (20 blocks of 20 cycles each). In some runs acquisition was stopped when the standard error of the ^{40}Ca/^{44}Ca ratios became smaller than 0.002.

We found an average ^{40}Ca/^{44}Ca for modern marine skeletal carbonates (corals and sclerosponges) of 47.163 ± 0.01 (2σ, $n = 7$). This value is not significantly different (ANOVA, $p = 0.15$) from the average Devonian/Silurian ratio of 47.159 ± 0.01 (2σ, $n = 9$), measured on brachiopods from the Wenlock, Ludlow, Lochkovian, Emsian, Eifelian, Givetian, Frasnian (2 specimens), and Famennian. Both ^{40}Ca/^{44}Ca values agree with the modern marine carbonate (*Tridacna*) value of 47.168 ± 0.01 determined by Nelson and McCulloch (1989), and the MORB ratios of 47.155 ± 0.001 and 47.168 ± 0.009 of Kreissig and Elliott

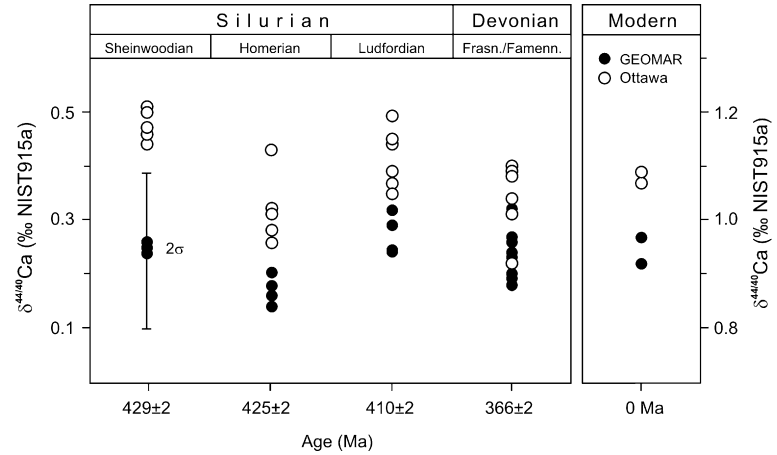

Fig. 1. Measured $\delta^{44/40}$Ca values of coeval, Silurian, Devonian and modern brachiopods as determined at IFM-GEOMAR (black circles) and Ottawa/Carleton (open circles) laboratories. Error bar represents the average 2σ of ±0.15‰. The samples of modern brachiopods (*Terebratalia transversa*) were collected from San Juan Island, NW Pacific (cf. Tomašových, 2004; Gussone et al., 2005; Farkaš et al., 2007).

(2005) and Nelson and McCulloch (1989), respectively. This confirms the conclusion of the latter study, that modern seawater has a radiogenic Ca excess that is indistinguishable from the mantle (MORB) signature. Our Early Paleozoic $^{40}Ca/^{44}Ca$ ratio indicates that this was also the case in the early Phanerozoic.

3. RESULTS

The measured $\delta^{44/40}Ca$ values of brachiopods (see Appendix, Table EA-4), complemented by literature data (Table EA-5), are plotted as a function of time in Fig. 2. The Phanerozoic $\delta^{44/40}Ca$ record of marine carbonates ($n = 419$) and phosphates ($n = 22$) exhibits a temporal variation with a magnitude of about 2‰, from −0.5‰ to 1.5‰. Overall, the compiled $\delta^{44/40}Ca$ dataset defines a rising trend, from ~0.4‰ at the beginning of the Ordovician to ~1‰ at present, with a major positive excursion at the Carboniferous/Permian transition and a substantial scatter, up to ~2‰, during the Cretaceous. In addition, there are indications of several, mostly negative, short-term oscillation superimposed on the general rising trend.

4. DISCUSSION

While the $\delta^{44/40}Ca$ of marine carbonates and phosphates are assumed to reflect primarily the isotope composition of seawater (De La Rocha and DePaolo, 2000; Schmitt et al., 2003a; Heuser et al., 2005), ambient temperature (Nägler et al., 2000; Hippler et al., 2002; Gussone et al., 2004), mineralogy of precipitates (Gussone et al., 2005) and kinetics (Lemarchand et al., 2004; Gussone et al., 2005) also play a role. In order to reconstruct the calcium isotope composition of Phanerozoic seawater it is essential to know the isotope fractionation factor ($\alpha_{CC/SW}$) between seawater and the recording phase (e.g. brachiopod calcite) as well as its dependence on temperature.

4.1. Fractionation factors ($\alpha_{CC/SW}$) and their sensitivity to temperature

The compiled $\delta^{44/40}Ca$ dataset comprises samples with either calcitic or phosphatic mineralogies, the former includes brachiopods, belemnites, foraminifera and rudists, and the latter marine authigenic phosphates.

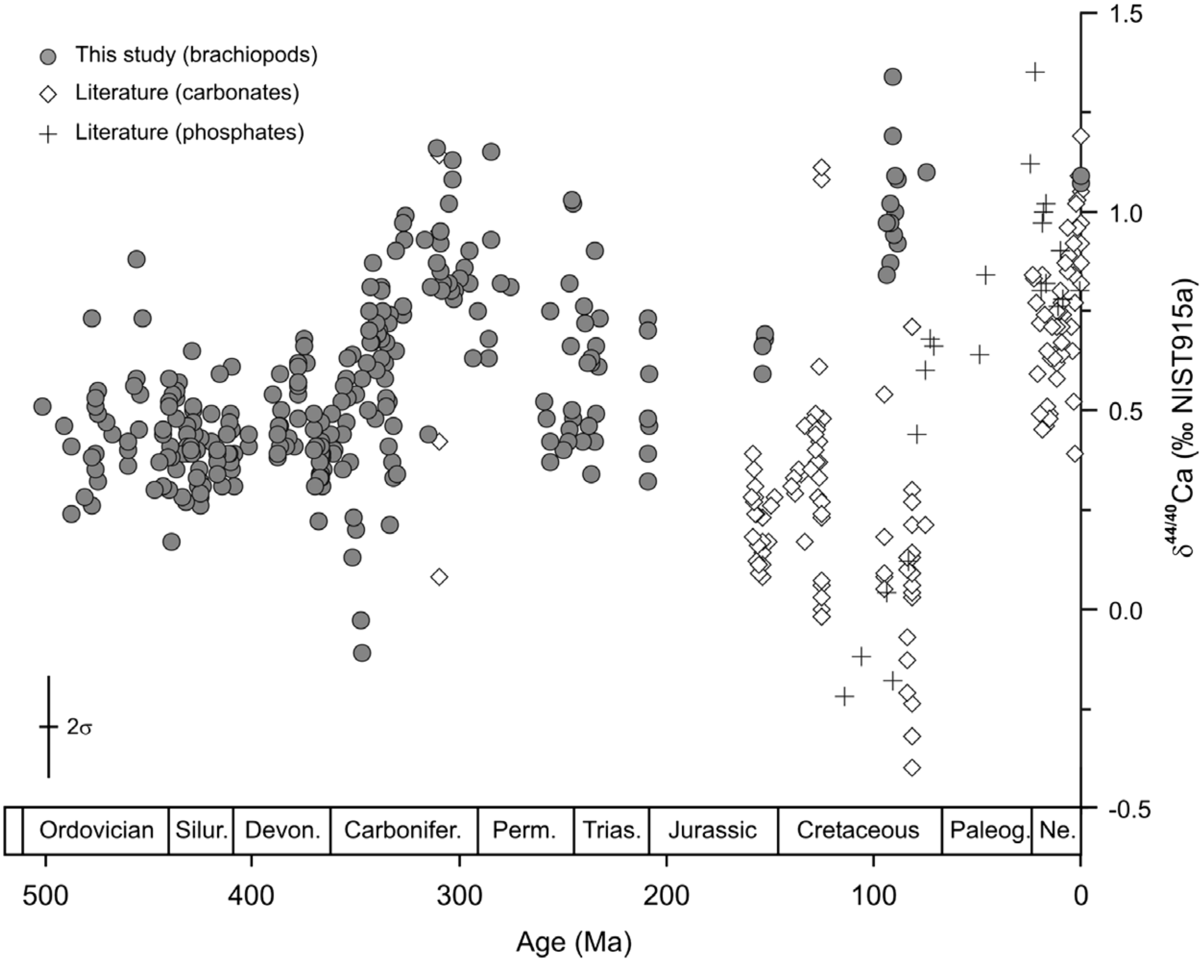

Fig. 2. Measured $\delta^{44/40}Ca$ values of Phanerozoic brachiopods (grey circles, $n = 280$; this study), complemented by literature data from marine carbonates (open diamonds, $n = 139$) and authigenic phosphates (black crosses, $n = 22$). The literature data are from the following sources: Heuser et al. (2005), Steuber and Buhl (2006), Farkaš et al. (2007), Schmitt et al. (2003a) and Soudry et al. (2004). Time scale from Harland et al. (1990).

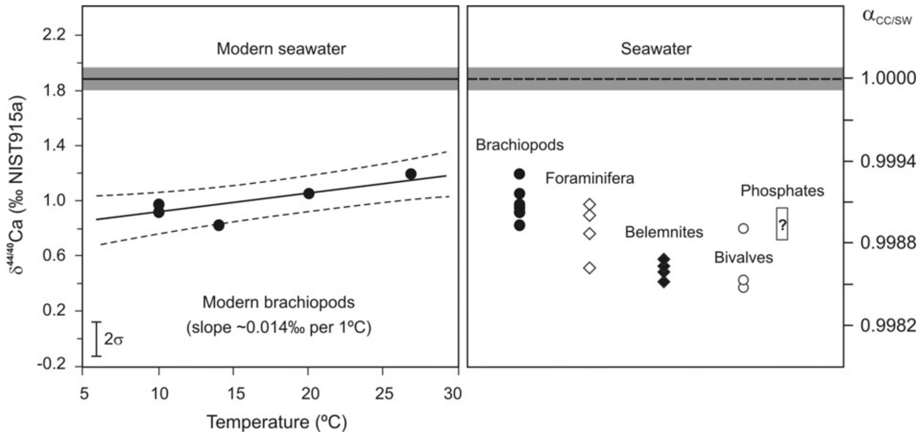

Fig. 3. Left panel: $\delta^{44/40}$Ca of modern brachiopod calcite as a function of seawater temperature (data from Gussone et al., 2005). Solid/dashed horizontal lines represent the calcium isotope composition of modern seawater of 1.88‰ and the gray bands indicate the 2σ uncertainty of ±0.04‰ (Hippler et al., 2003). Right panel: calcium isotope fractionation factors (α_{CC-SW}) between seawater (SW) and the following solid phases (CC): skeletal calcite of brachiopods, foraminifera (Heuser et al., 2005), belemnites (Farkaš et al., 2007), bivalves (Steuber and Buhl, 2006) and marine phosphates (Schmitt et al., 2003a).

The fractionation factor, $\alpha_{CC/SW}$, can be calculated from the calcium isotope composition of seawater and the corresponding recording phase using the following relation:

$$\alpha_{CC/SW} = \left(\delta^{44/40}\mathrm{Ca}_{CC} + 1000\right) \Big/ \left(\delta^{44/40}\mathrm{Ca}_{SW} + 1000\right) \qquad (1)$$

where $\delta^{44/40}\mathrm{Ca}_{CC}$ and $\delta^{44/40}\mathrm{Ca}_{SW}$ represent the calcium isotope compositions of the recording phase and seawater, respectively (Heuser et al., 2005).

For brachiopods, the fractionation factor was determined on modern specimens (*Terebratalia*, *Thecidellina*, *Waltonia* sp.) and these yielded the mean $\alpha_{CC/SW}$ of ~0.99915 and a weak temperature dependency of ~0.014‰ °C^{-1} (Fig. 3) (Gussone et al., 2005; see also Farkaš et al., 2007). For belemnites, we used $\alpha_{CC/SW}$ of ~0.99860 (Fig. 3) inferred from samples of coeval Late Jurassic belemnites (*Hibolites* sp.) and brachiopods (*Lacunosella* sp.) that were collected from the same stratigraphic horizons (cf. Farkaš et al., 2007). The temperature sensitivity of belemnite $\delta^{44/40}$Ca is assumed to be weak, likely <0.02‰ °C^{-1}, judging from the statistically insignificant correlation between $\delta^{44/40}$Ca and δ^{18}O of belemnite calcite (Farkaš et al., 2007). For foraminifera, the $\alpha_{CC/SW}$ was calculated from modern, or the most recent, planktonic foraminifers (*Globigerinoides tribolus*, *Globigerina bulloides*) that yielded the mean $\alpha_{CC/SW}$ of ~0.99905 and a weak $\delta^{44/40}$Ca-temperature gradient of <0.02‰ °C^{-1} (Gussone et al., 2003; Heuser et al., 2005). For rudist bivalves, the fractionation factor has not yet been constrained experimentally and we therefore adopted $\alpha_{CC/SW}$ of modern oysters (*Ostrea* sp.) of ~0.99850 (Steuber and Buhl, 2006). The sensitivity of rudist $\delta^{44/40}$Ca to temperature is expected to be high, possibly up to 0.25‰ °C^{-1} (Immenhauser et al., 2005; see, however, discussion in Steuber and Buhl, 2006), which may result in significantly larger scatter and uncertainty for the reconstructed calcium isotope composition of Cretaceous seawater.

For marine phosphates, the $\alpha_{CC/SW}$ is assumed to be close to 0.9991 based on the analysis of a Pleistocene (0.5 Ma) sample (Schmitt et al., 2003a). This value, however, should be taken with caution because marine authigenic phosphates are products of early diagenesis, and thus calcium used for their formation originates not only from seawater but also from the dissolution of carbonates in the sediment (Soudry et al., 2004). The latter have significantly lighter $\delta^{44/40}$Ca compared to seawater. The $\delta^{44/40}$Ca-temperature gradient of phosphates is considered to be weak, likely less than 0.02‰ °C^{-1}, as indicated by poor correlation between $\delta^{44/40}$Ca and δ^{18}O of Miocene phosphates (Schmitt et al., 2003a).

A summary showing the calcium isotope fractionation factors, $\alpha_{CC/SW}$, for the above mentioned recording phases, with the corresponding $\delta^{44/40}$Ca-temperature gradients, is presented in Table 2.

Table 2
The calcium isotope fractionation factors between seawater and skeletal calcite ($\alpha_{CC/SW}$) of brachiopods, belemnites, foraminifera and bivalves as well as marine authigenic phosphates

Material/ recording phase	$\alpha_{CC/SW}$	1000 ln ($\alpha_{CC/SW}$) (‰)	$\delta^{44/40}$Ca-temperature gradient (‰ °C^{-1})
Brachiopods	0.99915[a]	−0.85	<0.015
Belemnites	0.99860[b]	−1.40	< 0.020
Foraminifera (*G. tribolus*)	0.99906[c]	−0.94	<0.020
Bivalves: oysters (rudists)	0.99850[d]	−1.50	~0.250[f]
Authigenic phosphates	0.99910[e]	−0.90	<0.020

[a] Gussone et al. (2005) and Farkaš et al. (2007).

[b] Farkaš et al. (2007).

[c] Heuser et al. (2005).

[d] Steuber and Buhl (2006).

[e] Schmitt et al. (2003a).

[f] Based on data of rudist bivalve (*Vaccinites* sp.) of Immenhauser et al. (2005).

4.2. Reconstruction of calcium isotope composition of Phanerozoic seawater

The calcium isotope composition of paleo-seawater was calculated from the compiled $\delta^{44/40}$Ca dataset of marine carbonates and phosphates (Fig. 2) and the corresponding fractionation factors $\alpha_{CC/SW}$ (Table 2), using Eq. (1). The reconstructed Phanerozoic $\delta^{44/40}Ca_{SW}$ curve (Fig. 4) exhibits an increasing trend from about 1.3‰ at the beginning of the Ordovician to about 2‰ at present. Superimposed on this overall trend is a major long-term (~70 Ma) positive excursion, from the Early Carboniferous to Early Permian, and several, mostly negative, short-term excursions with a typical duration on the order of 5–10 Ma.

In general, the secular $\delta^{44/40}Ca_{SW}$ trend exhibits a rather uniform scatter of about ±0.25‰, except for the Late Cretaceous where $\delta^{44/40}Ca_{SW}$ data spread is from ~0.7‰ to 2.2‰. The predominant scatter of ±0.25‰ likely results from a combination of several variables such as: (i) the external reproducibility of our measurements of ±0.15‰; (ii) the effect of temperature on the calcium isotope composition of skeletal calcite of about 0.02‰ °C^{-1}; (iii) minor enrichments in radiogenic ^{40}Ca of less than 0.2‰ (DePaolo, 2004); and in some cases we cannot exclude the possibility that the calcium isotope composition of the samples has been compromised by post-depositional processes.

To smooth natural fluctuations observed in the experimental $\delta^{44/40}Ca_{SW}$ record we applied a moving average filter with a 10 point window to illustrate the secular $\delta^{44/40}Ca_{SW}$ trend for most of the Paleozoic and parts of the Mesozoic and Cenozoic (Fig. 5). Note, however, that the phosphate data were excluded from this exercise, as inclusion of the phosphate data generates a significantly different $\delta^{44/40}Ca_{SW}$ record during the Cretaceous, which will be discussed below. We have also examined other scenarios where the smoothing was calculated using a 3-, 5-, 15- and 25-point averaging window, yet it was found that the overall $\delta^{44/40}Ca_{SW}$ trends do not change much with varying resolution (for details see the auxiliary material, Fig. EA-1).

The statistical filtering confirmed a presence of several higher-order oscillations with a typical magnitude of about 0.4‰ and duration of 5–10 Ma that are superimposed on

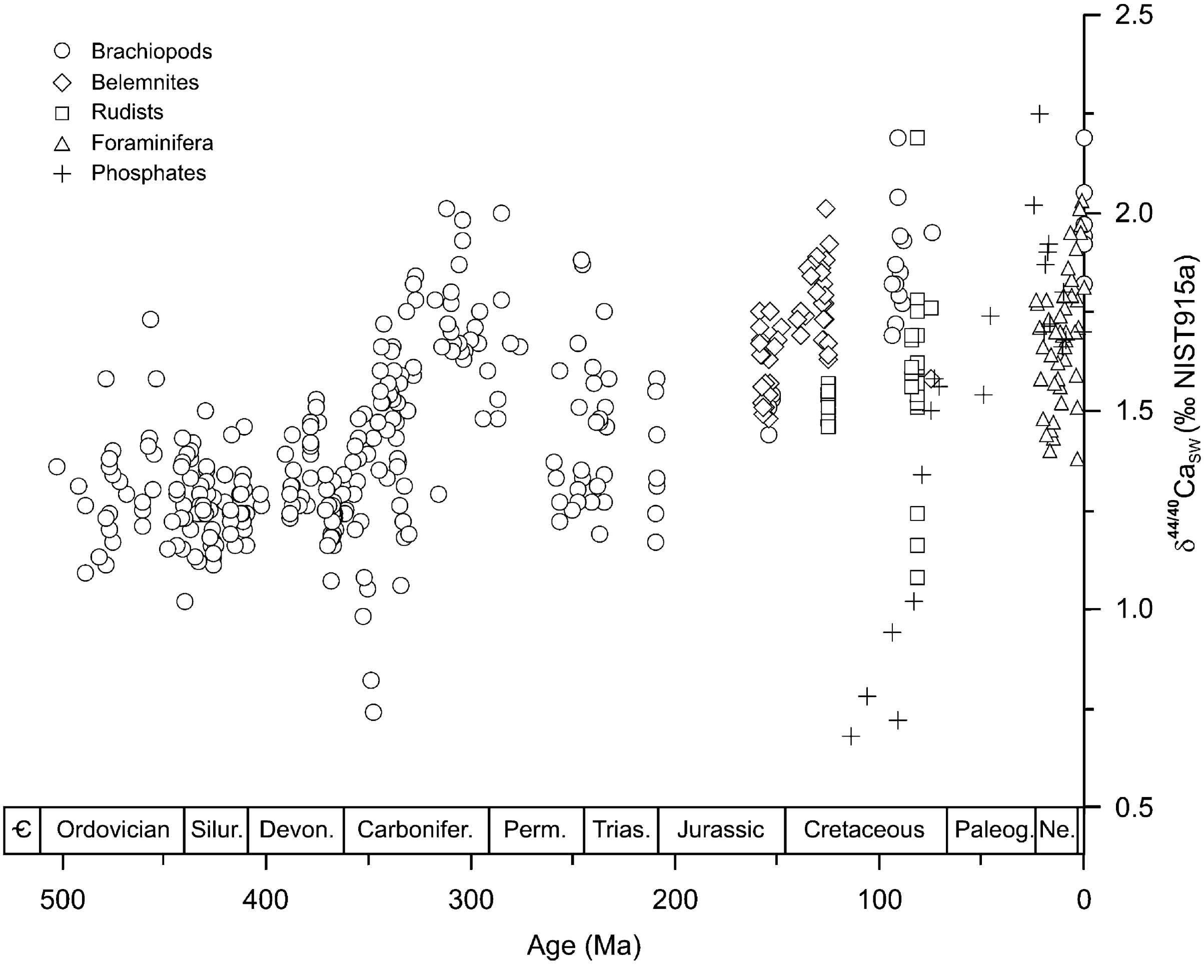

Fig. 4. The compilation of our and literature data ($n = 419$) showing the reconstructed calcium isotope evolution of Phanerozoic seawater ($\delta^{44/40}Ca_{SW}$) based on data of brachiopods (open circles), belemnites (open diamonds), rudists (open squares), foraminifera (open triangles) and marine phosphates (crosses). The $\delta^{44/40}Ca_{SW}$ trend was calculated using the following fractionation factors ($\alpha_{CC/SW}$): brachiopods = 0.99915; belemnites = 0.99860; rudists = 0.99850; foraminifera = 0.99905; and phosphates = 0.99910. Time scale from Harland et al. (1990).

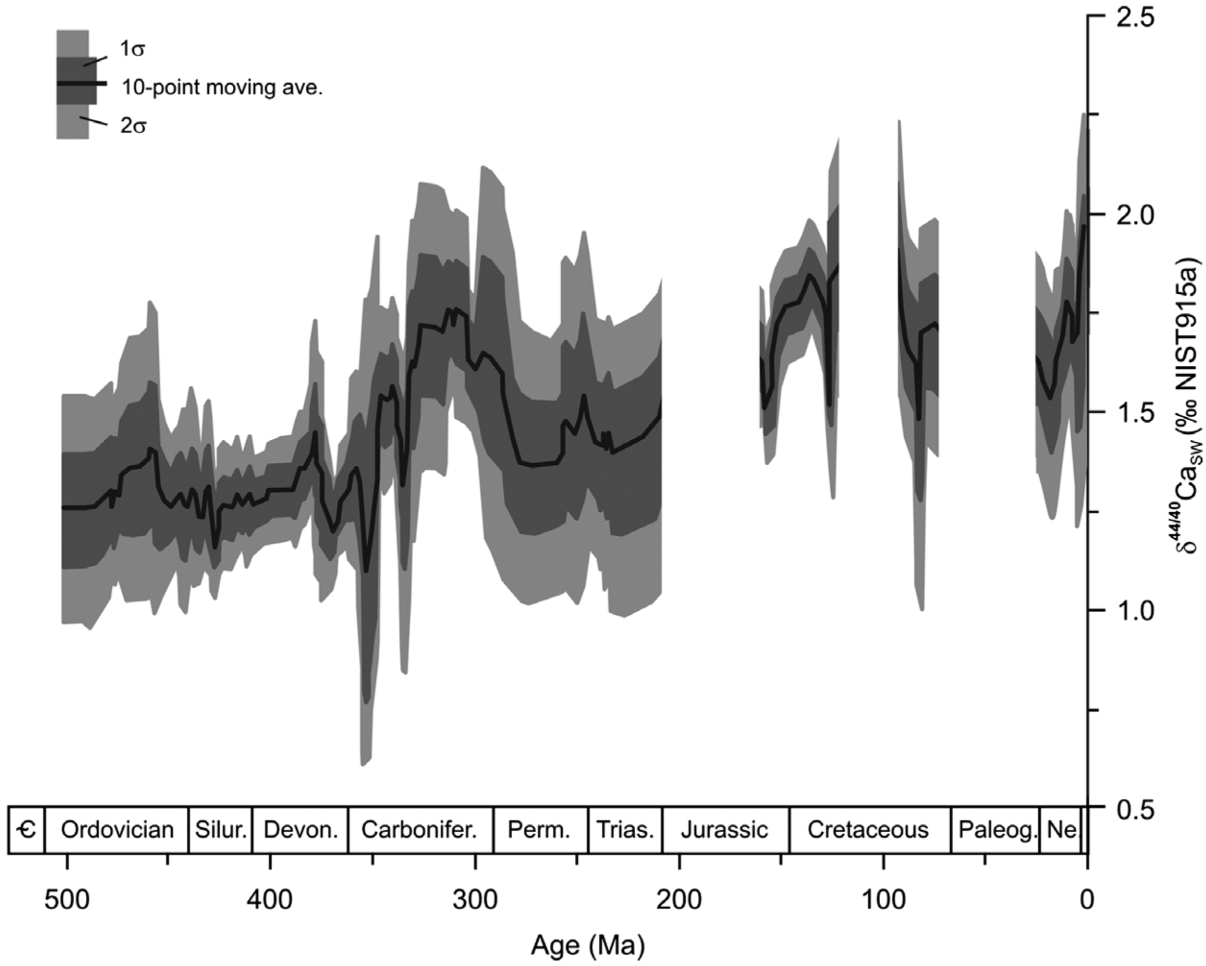

Fig. 5. Smoothed Phanerozoic $\delta^{44/40}Ca_{SW}$ trend based only on data of marine skeletal carbonates ($n = 397$). The moving average trend (solid line) is calculated using a 10-point smoothing window. The dark and light bands around the moving average trend represent 68% ($\pm 1\sigma$) and 95% ($\pm 2\sigma$) confidence intervals, respectively. Time scale from Harland et al. (1990).

the overall $\delta^{44/40}Ca_{SW}$ trend (Fig. 5). There are indications of several short-term positive peaks, the most apparent in the Middle Ordovician, Middle/Late Devonian and Late Permian (Fig. 5). The negative excursions are however much more common and the most pronounced are documented in the Middle Silurian, Late Devonian, Early Carboniferous, Late Jurassic, Early/Late Cretaceous and Neogene (Fig. 5). The magnitudes of these short-term excursions vary from less than ~0.2, (e.g. Middle Silurian) up to more than ~0.5‰ (e.g. Early Carboniferous). Note that these values represent minimal estimates as they are derived from the smoothed dataset (Fig. 5).

Taking the Carboniferous $\delta^{44/40}Ca_{SW}$ trend as an example, the approximate duration and magnitude of the short-term excursions can be constrained (Fig. 6). The calcium isotope composition of Early Carboniferous (Mississippian) seawater, based on 60 brachiopod samples, exhibits a gradually increasing trend from the Early Tournaisian $\delta^{44/40}Ca_{SW}$ of ~1.3‰ to Late Serpukhovian values of ~1.75‰. Superimposed on this trend are two pronounced short-term negative excursions with $\delta^{44/40}Ca_{SW}$ minima dated at ~352 Ma (Tournaisian/Visean) and ~334 Ma (Visean/Serpukhovian). The approximate duration of these excursions is about 10 ± 2 Ma and the magnitudes are up to 0.7‰, the latter estimate based on the original (non-smoothed) $\delta^{44/40}Ca_{SW}$ dataset. The calcium isotope composition of the Late Carboniferous (Pennsylvanian) seawater is based on a much smaller dataset ($n = 23$) and it shows a rather constant $\delta^{44/40}Ca_{SW}$ trend with a mean of ~1.7‰.

4.3. Causes and implications of secular variations in Phanerozoic $\delta^{44/40}Ca_{SW}$ record

4.3.1. Global calcium cycle from isotope perspective

The $\delta^{44/40}Ca_{SW}$ value of the modern ocean of 1.88 ± 0.1‰ is globally homogeneous and independent of depth (Schmitt et al., 2001; Hippler et al., 2003), as expected from the long residence time of calcium in seawater, ~1 Ma, compared to the average mixing time of the ocean of ~1500 years (Broecker and Peng, 1982).

The average $\delta^{44/40}Ca$ of the primary source of calcium to the ocean, the continental river flux, is not accurately known but it is assumed to be close to 0.8 ± 0.2‰ (Zhu

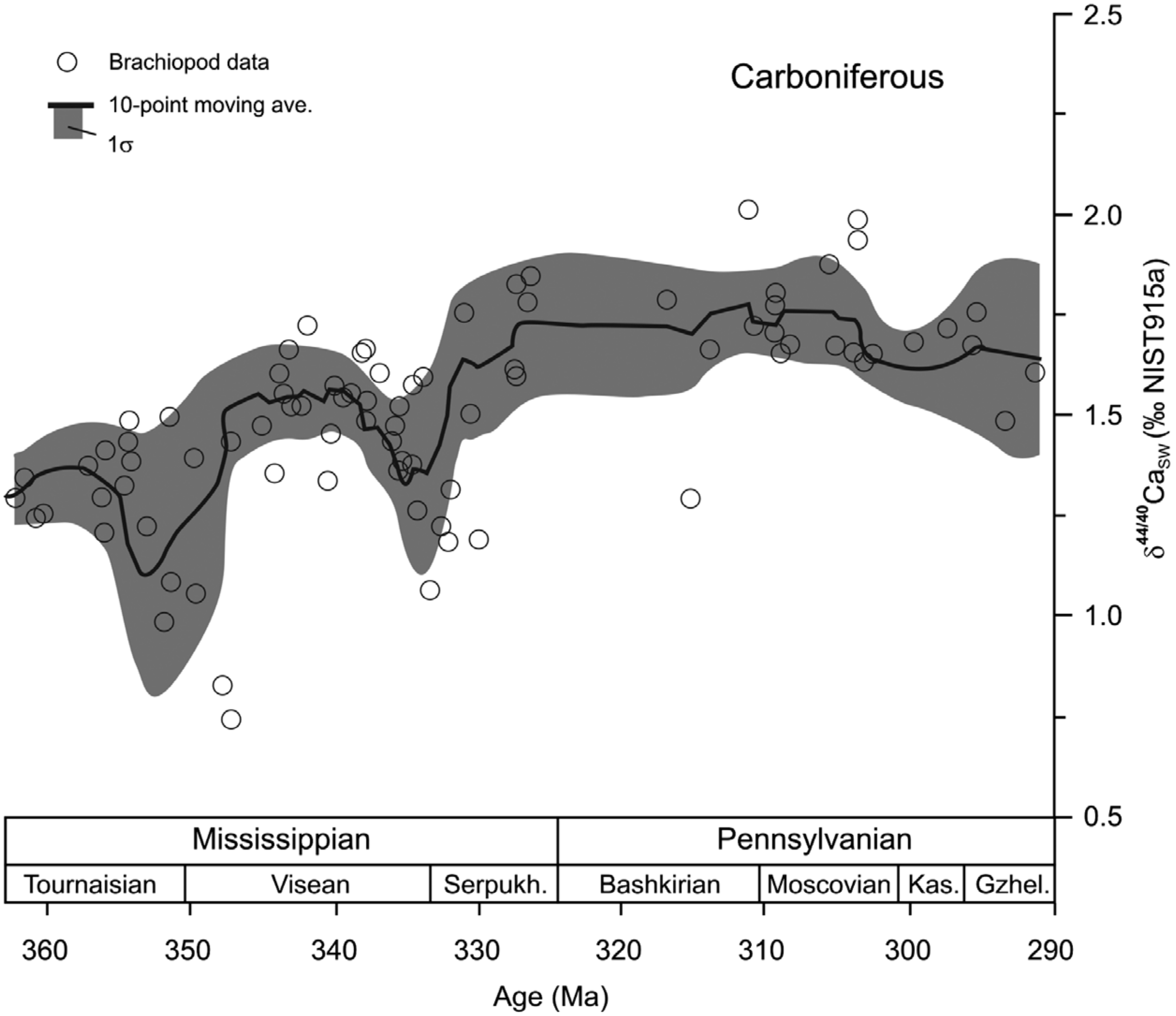

Fig. 6. The Carboniferous $\delta^{44/40}Ca_{SW}$ trend, based on brachiopod data ($n = 83$), showing two short-term negative excursions during the Mississippian. The smoothed trend, solid line with shaded area (±1σ), is calculated from the original $\delta^{44/40}Ca_{SW}$ dataset (open circles) using a 10-point moving average. Time scale from Harland et al. (1990).

and Macdougall, 1998; Schmitt et al., 2003b; Heuser et al., 2005; Tipper et al., 2006). For smaller catchments, however, this value may vary significantly, from 0.5‰ to 1‰ (Schmitt et al., 2003b; Wiegand et al., 2005), depending on the net effect of biogeochemical processes, such as downstream precipitation of carbonates (Tipper et al., 2006) and/or recycling of soil calcium by vegetation (Schmitt et al., 2003b; Wiegand et al., 2005). The isotope signature of calcium supplied to the ocean by hydrothermal solutions at mid-ocean ridges is estimated to be close to ∼0.9 ± 0.2‰ (Schmitt et al., 2003b; Amini et al., 2006) and is not expected to change with time. The low-temperature diffuse calcium flux at mid-ocean ridges is likely more depleted in ^{44}Ca than the discrete high-temperature flux, due to redissolution of isotopically light hydrothermal anhydrite. Mass balance considerations point to a general hydrothermal $\delta^{44/40}$Ca of about 0.7‰ (Berner and Berner, 1996; Amini et al., 2006). Calcium released to the ocean during the dolomitization of marine carbonates is expected to be significantly lighter, with the mean $\delta^{44/40}$Ca of about 0.3 ± 0.2‰ (Artemov et al., 1967; Böhm et al., 2005; Heuser et al., 2005).

The major sink for the oceanic calcium, neritic and pelagic carbonate sedimentation, has $\delta^{44/40}$Ca uniform at ∼0.95 ± 0.3‰ for calcite (DePaolo, 2004; Gussone et al., 2005; Heuser et al., 2005), at ∼0.4 ± 0.2‰ for aragonite (Böhm et al., 2002; Gussone et al., 2003, 2005), and around 0.7 ± 0.2‰ for mineralization characterized by biological fractionation, e.g. in coccoliths and corals (Böhm et al., 2006; Gussone et al., 2006). The $\delta^{44/40}$Ca of marine carbonates is also dependent on temperature (Nägler et al., 2000; Hippler et al., 2002) and carbonate ion concentration in the surface ocean (Lemarchand et al., 2004; Gussone et al., 2005), nevertheless, modern biogenic carbonates exhibit only a weak sensitivity to these variables (Gussone et al., 2003, 2005; DePaolo, 2004; Heuser et al., 2005).

The isotope composition of marine evaporites, specifically gypsum and anhydrite, is very variable with values ranging from 0.2‰ to 1.7‰, which is likely due to Rayleigh fractionation associated with rapid precipitation (Hensley, 2006). However, gypsum formed in marginal marine basins or salt-pans shows only little isotope fractionation with respect to the dissolved calcium in seawater (1.88‰) (Yang et al., 2006) and therefore we assume the upper limit of the measured values (1.7‰) to be the most representative for marine evaporites. Anhydrites formed during the hydrothermal alteration of oceanic crust have generally lighter signatures of −0.5‰ to 0.7‰, because they are precipitated from hydrothermal fluids with low $\delta^{44/40}$Ca values (Hensley, 2006).

Based on the above isotope compositions of the major sources and sinks of calcium to the modern ocean, and their corresponding fluxes (cf. Wallmann, 2001; DePaolo, 2004), the present-day seawater is close to steady state with respect to calcium isotopes and concentrations (Hardie, 1996; Skulan et al., 1997; De La Rocha and DePaolo, 2000; Schmitt et al., 2003b; Berner, 2004), which however was not always the case in geological history.

4.3.2. Simulating Phanerozoic evolution of seawater calcium isotope composition ($\delta^{44/40}Ca_{SW}$) and concentrations

To simulate the Phanerozoic evolution of calcium seawater concentrations and isotope composition we used a model of coupled calcium/carbon/magnesium global cycles (Wallmann, 2001, 2004; Hansen and Wallmann, 2003; Heuser et al., 2005). The model uses the Phanerozoic ^{87}Sr/^{86}Sr record of Veizer et al. (1999) to calculate seafloor spreading and subduction rates (Wallmann, 2004).

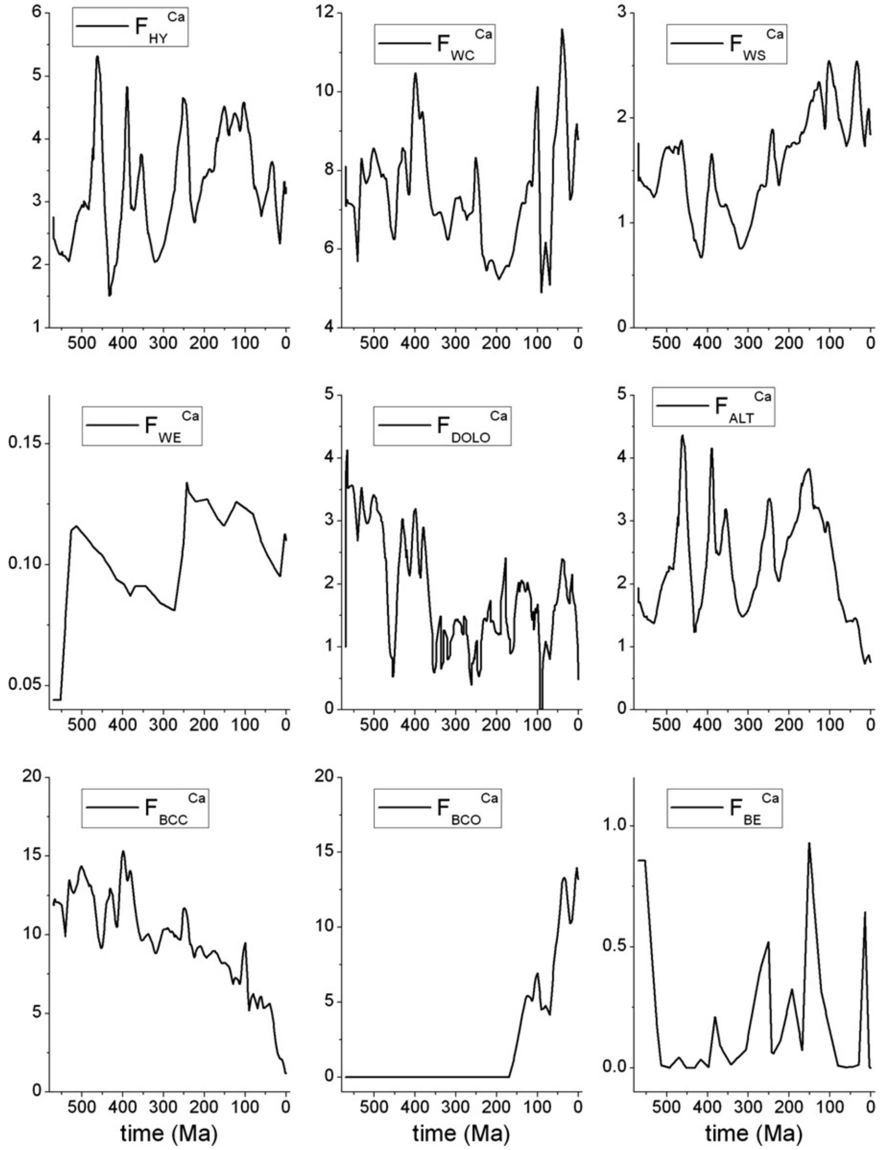

Fig. 7. Calcium fluxes applied in the model (in Tmol Ca yr^{-1}). $F_{HY}{}^{Ca}$: hydrothermal Ca input into the ocean; $F_{WC}{}^{Ca}$: Ca released during carbonate weathering; $F_{WS}{}^{Ca}$: Ca released via silicate weathering; $F_{WE}{}^{Ca}$: Ca released during evaporite weathering; $F_{DOLO}{}^{Ca}$: Ca released during dolomitization of marine carbonates; $F_{ALT}{}^{Ca}$: seawater Ca removed from the ocean during the alteration of oceanic crust; $F_{BCC}{}^{Ca}$: seawater Ca fixed in carbonates deposited on the continental shelf; $F_{BCO}{}^{Ca}$: seawater Ca fixed in pelagic carbonates; $F_{BE}{}^{Ca}$: seawater Ca fixed in marine evaporites. The corresponding equations for individual fluxes of calcium are available in Appendix EA-2 (Table EA-2).

Dolomite formation rates are calculated from the record of oceanic Mg/Ca ratios (Lowenstein et al., 2001; Horita et al., 2002; Ries, 2004; Steuber and Rauch, 2005). The model is described in detail in the auxiliary material (see Appendix EA-2).

For the mass balance of the oceanic calcium cycle the model considers release of calcium into the oceans through hydrothermal circulation at mid-ocean ridges $\left(F_{HY}{}^{Ca}\right)$, dolomitization of carbonates deposited on the continental shelf $\left(F_{DOLO}{}^{Ca}\right)$ and via continental weathering of carbonate $\left(F_{WC}{}^{Ca}\right)$, silicate $\left(F_{WC}{}^{Ca}\right)$ and evaporite $\left(F_{WE}{}^{Ca}\right)$ rocks. Calcium is removed from seawater through carbonate burial on the continental shelf $\left(F_{BCS}{}^{Ca}\right)$, pelagic carbonate deposition at the deep-sea floor $\left(F_{BCP}{}^{Ca}\right)$, evaporite accumulation $\left(F_{BE}{}^{Ca}\right)$ and the low-temperature alteration of oceanic crust $\left(F_{ALT}{}^{Ca}\right)$. All of these fluxes are considered in the model

$$\frac{dCa}{dt} = F_{HY}{}^{Ca} + F_{DOLO}{}^{Ca} + F_{WC}{}^{Ca} + F_{WS}{}^{Ca} + F_{WE}{}^{Ca} - F_{BCP}{}^{Ca} - F_{BCS}{}^{Ca} - F_{BE}{}^{Ca} - F_{ALT}{}^{Ca} \qquad (2)$$

The magnitudes (in Tmol of Ca yr^{-1}) of input and output fluxes of calcium to the ocean applied in the model are presented in Fig. 7. The corresponding equations for the calculation of individual calcium fluxes are available in Appendix EA-2 (Table EA-2) (see also Wallmann, 2001).

For the isotope model of the oceanic calcium cycle a characteristic $\delta^{44/40}$Ca signature is assigned to each flux (see Appendix EA-2, Table EA-3) to simulate the experimental $\delta^{44/40}Ca_{SW}$ record. Briefly, the isotope signatures of the calcium input fluxes from weathering of silicates $\left(F_{WS}{}^{Ca}\right)$ and evaporites $\left(F_{WE}{}^{Ca}\right)$ as well as the hydrothermal flux $\left(F_{HY}{}^{Ca}\right)$ were all kept constant at their modern $\delta^{44/40}$Ca levels. However, since the calcium isotope composition of marine carbonates changes with time, we applied a time dependent $\delta^{44/40}$Ca signature for the continental river flux derived from weathering of carbonate rocks $\left(F_{WC}{}^{Ca}\right)$ (Fig. 8), as well as for the dolomitization flux $\left(F_{DOLO}{}^{Ca}\right)$ as the calcium isotope composition of the latter is dependent on the source rock, i.e. marine carbonates.

The calcium isotope composition of the oceanic carbonate burial flux $\left(F_{BCS}{}^{Ca}, F_{BCP}{}^{Ca}\text{ and }F_{ALT}{}^{Ca}\right)$ is related to the composition of seawater, temperature, mineralogy (aragonite vs. calcite) and the carbonate ion concentration in the surface ocean as well as the metabolic mechanisms of a calcifying organism (Böhm et al., 2002, 2006; Gussone et al., 2003; Lemarchand et al., 2004; Gussone et al., 2005, 2006). Since the fractionation mechanisms involved in the formation of marine carbonates are poorly known, we used an inverse approach to determine the fractionation factor (α_{CARB}) of the oceanic carbonate burial flux needed to simulate the $\delta^{44/40}Ca_{SW}$ database presented in this paper, when the relevant calcium fluxes varied as shown in Figs. 7 and 8

$$\alpha_{CARB} = \frac{\left(\delta^{44/40}Ca_{CC} + 1000\right)}{\left(\delta^{44/40}Ca_{SW} + 1000\right)} = k_{CARB} \cdot \left(\delta^{44/40}Ca^{SW}{}_{MOD} - \delta^{44/40}Ca^{SW}{}_{DAT}\right) \qquad (3)$$

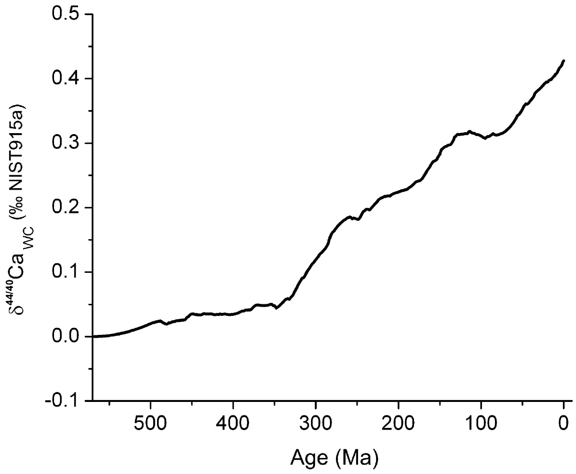

Fig. 8. Time dependent $\delta^{44/40}$Ca signature of carbonates subjected to weathering. Following Garrels and Mackenzie (1971), we assumed that the carbonate rocks have an average renewal time of 200 Ma, which was used to calculate the isotopic composition of weathering carbonates by a corresponding running mean through the carbonate fossils dataset presented in this paper.

The fractionation factor is proportional to the difference between the modeled and observed $\delta^{44/40}Ca_{SW}$ values. With this parameterization, α_{CARB} is automatically adjusted to minimize the difference between the two values for each time step. The kinetic constant k_{CARB} is set to a large value (50) so that the $\delta^{44/40}Ca_{SW}$ values calculated in the model (MOD) closely track the values documented in the geological record (DAT).

We explored two scenarios for the calculated α_{CARB} parameter to reconcile a large variability documented in Cretaceous $\delta^{44/40}Ca_{SW}$ values (Fig. 4). In the first scenario, α_{CARB} was varied to simulate the $\delta^{44/40}Ca_{SW}$ record based on skeletal carbonates, whereas in the second scenario it was adjusted to additionally match $\delta^{44/40}Ca_{SW}$ reconstructed from the phosphate data. The results of the modeling: concentrations of dissolved calcium and magnesium in seawater, partial pressures of CO_2 in the atmosphere, pH and total dissolved inorganic carbon in surface waters and the deep ocean, are presented in Fig. 9.

Fig. 10 shows a comparison between modeled and measured $\delta^{44/40}Ca_{SW}$ (two scenarios) as well as comparison between model results and independent data from the geological record, such as seawater calcium and magnesium concentrations (Lowenstein et al., 2001; Horita et al., 2002), the oceanic Mg/Ca ratios (Lowenstein et al., 2001; Horita et al., 2002; Ries, 2004; Steuber and Rauch, 2005) and the dominant mineralogy of marine skeletal carbonates in reefs (Kiessling, 2002).

4.3.3. Implications for chemical evolution of Phanerozoic seawater and the concept of 'calcite–aragonite seas'

Experimental data from fluid inclusions of primary marine halite (Lowenstein et al., 2001, 2003; Horita et al., 2002) indicate that the major ion composition of seawater has changed significantly over the Phanerozoic. Specifically, the concentrations of dissolved calcium and magnesium in

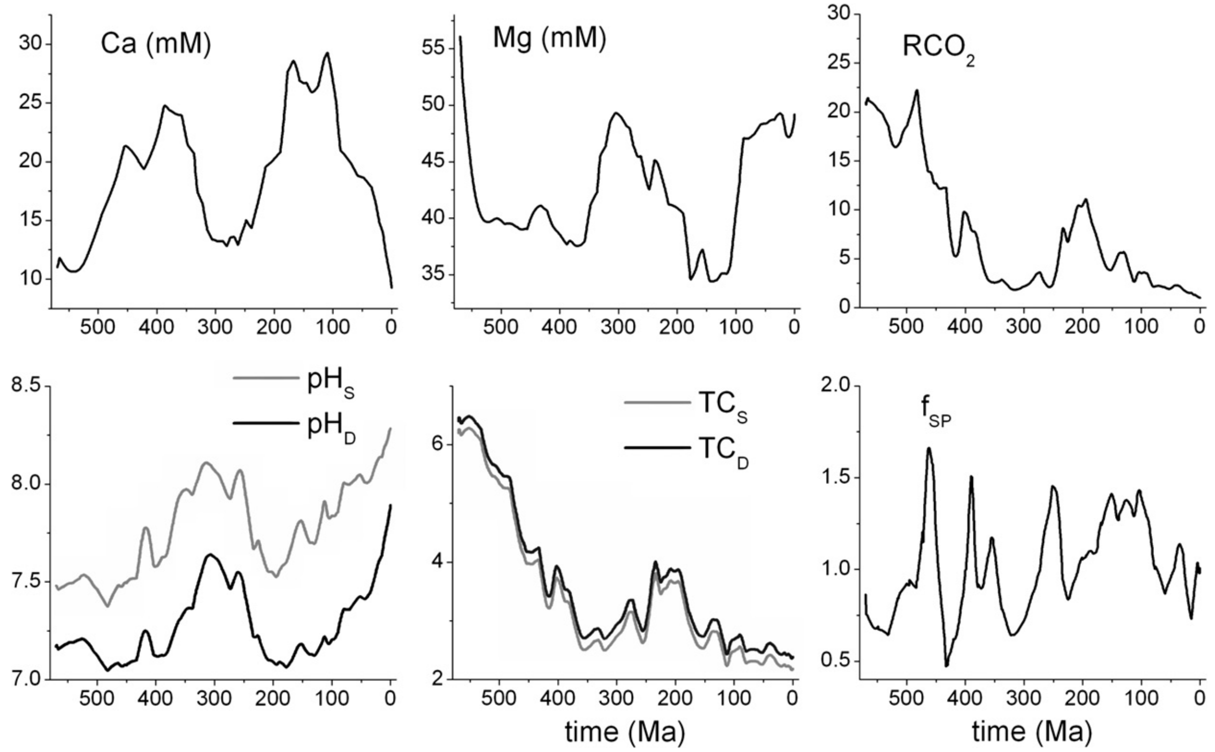

Fig. 9. Model results: concentrations of dissolved calcium and magnesium in seawater, partial pressures of CO_2 in the atmosphere normalized to the Quaternary value (RCO_2), pH in surface and deep waters, total dissolved inorganic carbon (TC) in surface and deep waters, spreading/subduction rate normalized to the modern value (f_{SP}).

seawater fluctuated in two long-term cycles and as mirror images of each other (Fig. 10). Consequently, the Mg/Ca ratio of Phanerozoic seawater also changed being mimicked by variations in mineral composition of marine skeletal and inorganic carbonates, so called 'calcite–aragonite seas' (Sandberg, 1983) (Fig. 10). These phenomena appear to be in phase with the stand of global sea level (Vail et al., 1977; Haq et al., 1987; Haq and Al-Qahtani, 2005) suggesting that the secular variations in chemical composition of seawater and the oscillating mineralogy of marine carbonates were primarily controlled by tectonic processes, specifically by changes in the rate of oceanic crust production and its hydrothermal alteration (Spencer and Hardie, 1990; Hardie, 1996; Stanley and Hardie, 1998; Steuber and Veizer, 2002).

The newly formed oceanic crust reacts with seawater exchanging dissolved magnesium for the igneous derived calcium that modifies the oceanic Mg/Ca ratio (Edmond et al., 1979), which in turn affects the mineralogy of marine carbonates (Sandberg, 1975; Hardie, 1996; Morse et al., 1997; Stanley and Hardie, 1998). At low-Mg/Ca ratio (<2) the dominant mineralogy of marine carbonates is low-Mg calcite, whereas during period of high oceanic Mg/Ca ratio the preference is given to aragonite and high-Mg calcite, as higher levels of magnesium in seawater inhibit the formation of low-Mg calcite (Berner, 1975; Morse et al., 1997).

The Paleozoic, Early Mesozoic and Neogene $\delta^{44/40}Ca_{SW}$ trends, and also the calculated α_{CARB}, are in phase with the variation in the oceanic Mg/Ca ratio and the alternating 'calcite–aragonite seas' (Fig. 10). In general, 'calcite seas' correspond to periods of light $\delta^{44/40}Ca_{SW}$ and high α_{CARB} values, whereas the trends are opposite for 'aragonite seas'. This correlation, however, does not hold true for the Late Mesozoic and Cenozoic $\delta^{44/40}Ca_{SW}$ and α_{CARB} trends reconstructed from data of skeletal carbonates (Fig. 10, scenario 1), but it holds relatively well for the coeval phosphate-based data (scenario 2). This inconsistency in the correlation pattern may be partly due to the poorly constrained calcium isotope composition of Mesozoic seawater compared to the much better defined Paleozoic and Neogene $\delta^{44/40}Ca_{SW}$ trends, the latter two based exclusively on brachiopod and foraminifera data, respectively.

With these qualifications, the major features of Phanerozoic $\delta^{44/40}Ca_{SW}$ trend can be explained by taking into account the difference between the calcium isotope composition of calcite vs. aragonite burial fluxes of the oceanic calcium, the former uniform at $\sim 0.95 \pm 0.3‰$ ($\alpha_{CC/SW} \approx 0.9991$) and the latter at $\sim 0.4 \pm 0.2‰$ ($\alpha_{CC/SW} \approx 0.9985$) (Fig. 10). Therefore, an increase in aragonite formation, i.e. 'aragonite seas', would preferentially remove light ^{40}Ca from seawater leaving the residual calcium in the ocean reservoir isotopically heavier, whereas an enhanced calcite formation, i.e. 'calcite seas', would shift $\delta^{44/40}Ca_{SW}$ towards isotopically lighter values. Thus, the long-term excursions in Phanerozoic $\delta^{44/40}Ca_{SW}$ record most likely reflect variable rates of aragonite vs. calcite production and deposition in the oceans over time.

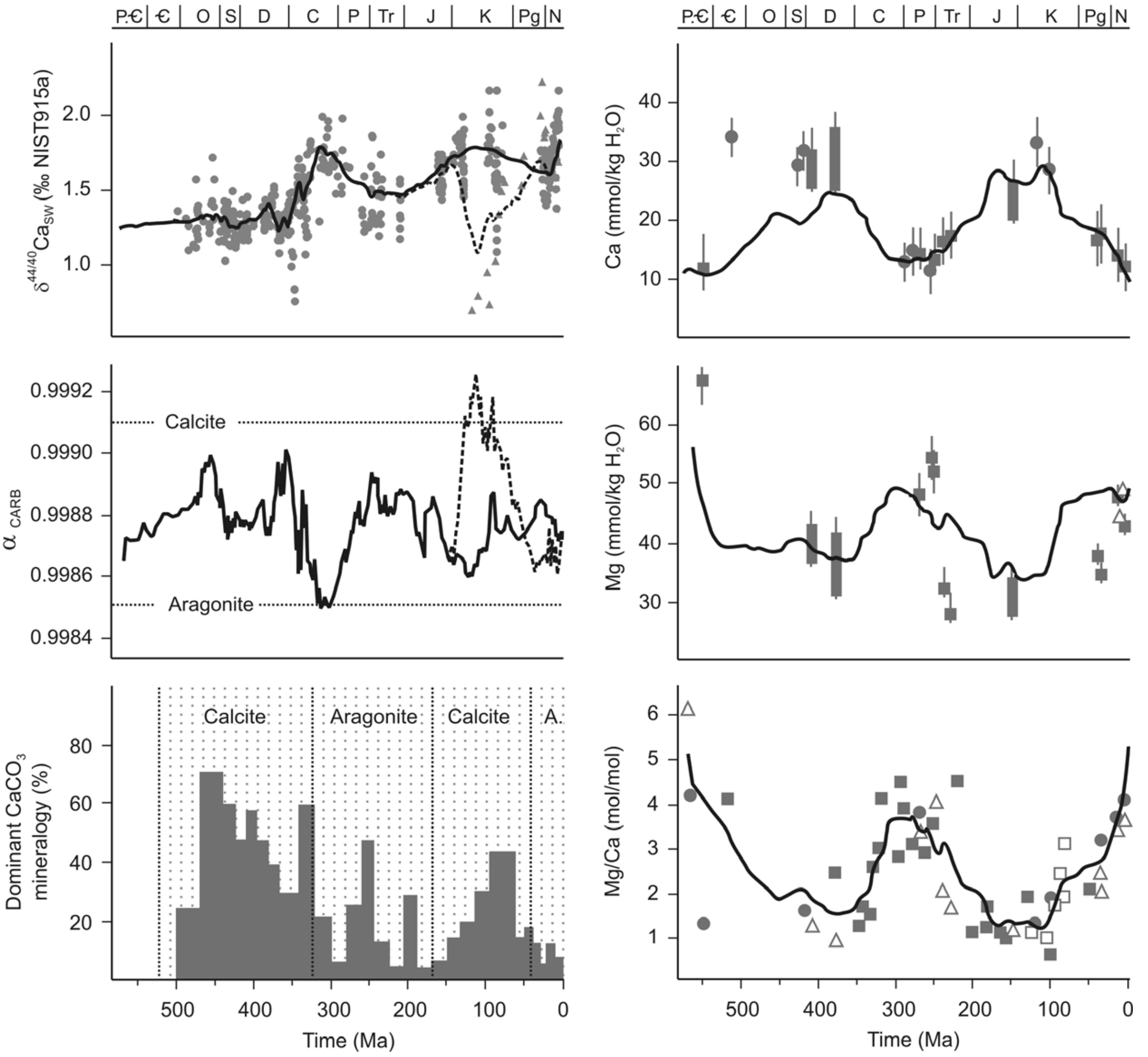

Fig. 10. Model results compared to independent data. Upper left panel: Phanerozoic $\delta^{44/40}Ca_{SW}$ trend as documented in the geological record (circles: carbonate data; triangles: phosphate data) and calculated in the model (solid line: scenario 1; dashed line: scenario 2). Middle left panel: Fractionation factor, α_{CARB}, for the formation of marine carbonates (shelf + pelagic + ocean crust) from seawater as calculated in the model (solid line: scenario 1; dashed line: scenario 2); dotted lines represent $\alpha_{CC/SW}$ of calcite and aragonite (Gussone et al., 2005). Lower left panel: dominant mineralogy of marine skeletal carbonates in reefs; shaded gray: calcite; dotted: aragonite + high-Mg calcite (Kiessling, 2002). Upper right panel: concentration of dissolved calcium in seawater documented in geological record (circles: Lowenstein et al., 2001; rectangles/squares: Horita et al., 2002) and calculated in the model. Middle right panel: concentration of dissolved magnesium in seawater documented in geological record (rectangles/squares: Horita et al., 2002; triangles: Zimmermann, 2000) and calculated in the model. Lower right panel: Mg/Ca ratio in seawater as documented in the geological record and calculated in the model. Solid circles: (Horita et al., 2002); solid squares: (Ries, 2004); open triangles: (Lowenstein et al., 2001); open squares: (Steuber and Rauch, 2005); solid line: model result.

In this point of view the above mentioned correlation breakdown in the Mesozoic and Cenozoic may be due to the expansion of coccolithophorids and modern scleractinian corals as major calcium carbonate producers (Kiessling, 2002; Falkowski et al., 2004). Calcification in both groups has been shown to produce a distinct Ca isotope signal ($\sim 0.7 \pm 0.2$‰, $\alpha_{CC(bio)/SW} \approx 0.9988$) that is independent of the skeletal mineralogy (Böhm et al., 2006; Gussone et al., 2006). Dominant marine $CaCO_3$ production by these organisms would therefore decouple biogenic Ca isotope fractionation from the 'aragonite–calcite sea' oscillations.

Other processes, such as post-depositional transformation of marine carbonates should not affect significantly the long-term calcium isotope budget of the oceans, as in submarine settings the transformation of aragonite to more stable calcite occurs more or less in situ (Melim et al., 2002; Munnecke and Westphal, 2005), resulting in no significant loss of calcium to seawater.

The results of the modeling exercise further support our interpretation as they show that the observed variation in Phanerozoic $\delta^{44/40}Ca_{SW}$ record cannot be explained solely by changing the magnitudes of input and output fluxes of calcium to the oceans. Other factors, such as the changing calcium isotope composition of the oceanic carbonate burial flux, i.e. the oscillating 'calcite–aragonite seas', must be taken into account.

In agreement with this explanation is the study of Steuber and Veizer (2002) that investigated the strontium contents of Phanerozoic skeletal carbonates (the same samples as in this study) and concluded that changes in mineralogy of marine carbonates and its effect on burial rates of strontium in the oceans provides the most consistent explanation for their experimental data.

A complementary explanation for the long-term excursions in the Phanerozoic $\delta^{44/40}Ca_{SW}$ trend is based on the effect of carbonate ion concentration, i.e. $[CO_3^{2-}]$, on calcium isotope fractionation of inorganic carbonates (Lemarchand et al., 2004). These authors showed that $\delta^{44/40}Ca$ of inorganic calcite precipitated from a solution with a high Ca/CO_3^{2-} ratio, such as seawater, is a linear function of dissolved $[CO_3^{2-}]$, which in turn controls the saturation state of the solution with respect to calcite and aragonite (Ω).

In theory, large shifts in $[CO_3^{2-}]$ of Phanerozoic surface oceans by up to a factor of 5, as proposed by the geochemical models of Locklair and Lerman (2005) and Tyrrell and Zeebe (2004), could have shifted the calcium isotope composition of marine carbonates by up to 0.7‰ (Gussone et al., 2005). Therefore the heavy $\delta^{44/40}Ca$ signatures of Late Carboniferous/Early Permian and Late Cenozoic brachiopods and foraminifera could be due to the higher $[CO_3^{2-}]$ of the contemporary surface oceans.

On the other hand, a generally weaker fractionation of the marine calcium carbonate production during these periods would have enriched seawater in light calcium, thus compensating for the carbonate ion effect on our $\delta^{44/40}Ca_{SW}$ recorders. In this case the seawater isotope shift would only be visible in $\delta^{44/40}Ca$ recorders that are not influenced by $[CO_3^{2-}]$, e.g. planktonic foraminifera (Gussone et al., 2003).

At this stage, we are not able to quantify the effect of carbonate ions on the reconstructed Phanerozoic $\delta^{44/40}Ca_{SW}$ trend as data constraining the $\delta^{44/40}Ca/CO_3^{2-}$ relationship for the individual recording phases and calcium carbonate producers are lacking. The only exceptions are the studies of Gussone et al. (2003) that showed no dependency of foraminiferal $\delta^{44/40}Ca$ (*Orbulina universa*) on ambient $[CO_3^{2-}]$, and of Gussone et al. (2006) who found a very weak negative dependency in the coccolithophorid *Emiliania huxleyi*. In addition, Langer (2005) found no dependency in another coccolithophorid, *Calcidiscus leptoporus*. These studies suggest that the effect of seawater carbonate ion concentration on the $\delta^{44/40}Ca$ of skeletal carbonates may be negligible, at least for calcifiers that use photosynthesis and control the carbonate chemistry in their calcifying fluids.

Finally, one of the most striking features of Phanerozoic $\delta^{44/40}Ca_{SW}$ trend are the short-term oscillations superimposed on the overall trend (Figs. 5 and 6). We speculate that these are related to periods of enhanced dolomite formation and/or to changes in the chemical composition of continental weathering flux, specifically short-term changes in Ca/HCO_3^- and Ca/SO_4^{2-} ratios of the global riverine flux, induced by variable rates of silicate vs. carbonate weathering on continents (Heuser et al., 2005).

A short-term negative excursion in $\delta^{44/40}Ca_{SW}$ record could be produced by enhanced rates of silicate weathering by sulphuric acid, e.g. during a period of enhanced volcanism. This would supply isotopically light calcium to the ocean without a proportional change in the carbonate ion flux, which would eventually shift $\delta^{44/40}Ca_{SW}$ to more negative values. Periods of increased sulfuric acid weathering should produce excursions in the marine sulfur isotope record, providing a possible test for the volcanic event hypothesis.

As to the explanation that is based on variable rates of dolomite formation, the resolution of the Mg/Ca record used to drive dolomitization in our model is unfortunately not sufficient to quantify events on a million year time scale. Future work on magnesium isotopes may provide high-resolution records of marine $\delta^{26}Mg$ to test whether dolomitization episodes influenced the calcium concentration and isotope composition of the oceans.

5. SUMMARY AND CONCLUSION

The reconstructed Phanerozoic $\delta^{44/40}Ca_{SW}$ trend, based on the analysis of 397 marine skeletal carbonates and 22 phosphates, shows a generally increasing trend from ~1.3‰ (NIST SRM 915a) at the beginning of the Ordovician to ~2‰ at present. Superimposed on this trend is a major long-term positive excursion from the Early Carboniferous to Early Permian as well as several short-term, mostly negative, oscillations during the Middle Silurian, Late Devonian, Early Carboniferous, Late Jurassic, Early/Late Cretaceous and Neogene. The radiogenic enrichment of ^{40}Ca on measured $\delta^{44/40}Ca$ values was examined on the samples of Silurian and Devonian brachiopods and was found indistinguishable from modern marine carbonates, indicating that a radiogenic Ca excess in the early Paleozoic oceans was similar to modern oceans.

The reconstructed Phanerozoic $\delta^{44/40}Ca_{SW}$ trend defines a rather consistent band of about ±0.25‰ that is most likely caused by several factors including (i) analytical uncertainty of ±0.15‰; (ii) the effect of temperature on $\delta^{44/40}Ca$ of skeletal calcite of ~0.02‰ °C^{-1}; (iii) minor enrichments in radiogenic ^{40}Ca of less than 0.2‰; and (iv) specific post-depositional history of the samples. The consistency in the scatter, however, indicates that the major isotope trends observed in this study are not caused by local factors like temperature variations or diagenesis but rather reflects secular changes in global $\delta^{44/40}Ca_{SW}$ signal. An exception is found in the Late Cretaceous where the scatter is much larger, possibly due to a higher sensitivity of rudist $\delta^{44/40}Ca$ to temperature and/or because the phosphate data may not faithfully reflect $\delta^{44/40}Ca_{SW}$. It is desirable that the calcium isotope composition of paleo-seawater should be based on comparable carrier phases, such as brachiopod and foraminiferal calcite that have only a weak $\delta^{44/40}Ca$-temperature gradient, <0.02‰ °C^{-1}.

Model simulations show that the observed variation in Phanerozoic $\delta^{44/40}Ca_{SW}$ record cannot be explained solely by varying the magnitudes of input and output fluxes of calcium to the ocean. The most likely complementary mechanism is the alternating mineralogy of marine skeletal carbonates, i.e. oscillating 'calcite–aragonite seas'.

Our results indicate that the calcium isotope budget of Phanerozoic oceans was ultimately controlled by tectonic processes, most likely via variable rates of oceanic crust production and its hydrothermal alteration. This modulated the oceanic Mg/Ca ratio that, in turn, controlled the dominant mineralogy of marine skeletal carbonates and hence the $\delta^{44/40}Ca_{SW}$. This interpretation is in accord with the proposition of Steuber and Veizer (2002) who concluded, from strontium concentrations in biological calcites, that the chemical composition of Phanerozoic seawater has been ultimately tectonically controlled. Other geochemical models available in literature that simulate the elemental cycling in the ocean–atmosphere system over the Phanerozoic, such as MAGic model of Arvidson et al. (2006a,b) also emphasize the sensitivity of seawater chemistry to variable rates of oceanic crust production and the intensity of seawater–basalt exchange reactions. In addition, the seawater trends calculated in our model (Fig. 9) are reasonably consistent with model outputs of Arvidson et al. (2006b), further supporting our interpretation of the measured calcium isotope data.

As to the possible causes of the short-term, mostly negative, oscillations that are superimposed on the long-term $\delta^{44/40}Ca_{SW}$ trend, we tentatively suggest that these are related to periods of enhanced dolomite formation and/or to temporal changes in the chemical composition of the continental riverine flux, specifically Ca/HCO_3^- and Ca/SO_4^{2-} ratios, induced by variable proportions of silicate vs. carbonate and CO_2 vs. SO_2 weathering rates.

ACKNOWLEDGMENTS

This study was supported by the Natural Science and Engineering Research Council of Canada and the Canadian Institute for Advanced Research (NSERC and CIAR research grants to J. Veizer). J. Farkaš was supported by the International Graduate Admission Scholarship of the University of Ottawa (2003–2007) and partially supported by Geological Society of America (2003 and 2004 GSA graduate student research grant). The contribution of F. Böhm and A. Eisenhauer was supported by the European Science Foundation (ESF) as part of the EUROclimate project (08) CASIOPEIA. Further support was provided by the 'Deutsche Forschungsgemeinschaft, DFG' Grants Ei272/13-1 (CATO) and Mu2352/1. Assistance with mass spectrometry and laboratory work of M. Wilk, L.A. Spencer, B. Cousens and S. Carr from Ottawa–Carleton Geoscience Centre (OCGC) and the Isotope Geochemistry and Geochronology Research Centre (IGGRC) is greatly acknowledged. M. Amini and B. Kisakürek kindly helped with measuring the IAPSO seawater standard at IFM-GEOMAR, and with discussions about hydrothermal calcium pathways and biogenic calcium fractionation. F. Hauff is thanked for keeping the stubborn Triton running at IFM-GEOMAR. Many thanks to N. Gussone and A. Heuser for their help with the Triton and calcium isotopes in general. This work is the IGGRC contribution No. 48.

APPENDIX A. SUPPLEMENTARY DATA

Supplementary data associated with this article can be found, in the online version, at doi:10.1016/j.gca.2007.09.004.

REFERENCES

Amini M., Eisenhauer A., Böhm F., Fietzke J., Bock B., Garbe-Schönberg D., Lackschewitz K. S. and Hauff F. (2006) Calcium isotope variations along the hydrothermal pathway. *Geophys. Res. Abstr.* **8**, Sref-ID: 1607-7962/gra/EGU06-A-08864.

Artemov Y. M., Strizhov V. P., Ustinov V. I. and Yaroshevskiy A. A. (1967) Possible isotope fractionation during dolomitization. *Geokhimiya* **5**, 519–529.

Arvidson R. S., Guidry M. and Mackenzie F. T. (2006a) The control of Phanerozoic atmosphere and seawater composition by basalt–seawater exchange reactions. *J. Geochem. Explor.* **88**, 412–415.

Arvidson R. S., Mackenzie F. T. and Guidry M. (2006b) MAGic: a Phanerozoic model for the geochemical cycling of major rock-forming components. *Am. J. Sci.* **306**, 135–190.

Berner R. A. (1975) The role of magnesium in the crystal growth of calcite and aragonite from seawater. *Geochim. Cosmochim. Acta* **39**, 489–504.

Berner E. K. and Berner R. A. (1996) *Global Environment: Water, Air, and Geochemical Cycles*. Prentice Hall, Upper Saddle River, NJ.

Berner R. A. (2004) A model for calcium, magnesium and sulfate in seawater over Phanerozoic time. *Am. J. Sci.* **304**, 438–453.

Böhm F., Eisenhauer A., Gussone N., Heuser A., Haase-Schramm A., Dietzel M., Reitner J. and Vacelet J. (2002) Fractionation of $^{44}Ca/^{40}Ca$ between aragonite and calcite. *Geochim. Cosmochim. Acta* **66**(Suppl. 1), A87.

Böhm F., Eisenhauer A., Heuser A., Kiessling W. and Wallmann K. (2005) Calcium isotope fractionation during dolomitization. *Schriftenr. Deutsch. Ges. Geowissensch.* **39**, 39.

Böhm F., Gussone N., Eisenhauer A., Dullo W.-Ch., Reynaud S. and Paytan A. (2006) Calcium isotope fractionation in modern scleractinian corals. *Geochim. Cosmochim. Acta* **70**, 4452–4462.

Broecker W. S. and Peng T.-H. (1982) *Tracers in the Sea*. Eldigo Press, New York, pp. 690.

Calner M., Jeppsson L. and Munnecke A. (2004) The Silurian of Gotland—part I: review of the stratigraphic framework, event stratigraphy, and stable carbon and oxygen isotope development—Erlanger geologische Abhandlungen, Sb**5**, 113–131.

De La Rocha C. L. and DePaolo D. J. (2000) Isotopic evidence for variations in the marine calcium cycle over the Cenozoic. *Science* **289**, 1176–1178.

DePaolo D. J. (2004) Calcium isotopic variations produced by biological kinetic radiogenic and nucleosynthetic processes. In *Geochemistry of Non-traditional Stable Isotopes*, vol. 55 (eds. C. M. Johnson, B. L. Beard and F. Albarede). Mineralogical Society of America and Geochemical Society, Washington, DC, pp. 255–288 (Rev. Mineral. Geochem.).

Dickson J. A. D. (2002) Fossil echinoderms as a monitor of the Mg/Ca ratio of Phanerozoic oceans. *Science* **298**, 1222–1224.

Edmond J. M., Measures C., McDuff R. E., Chan L. H., Collier R., Grant B., Gordon L. I. and Corliss J. B. (1979) Ridge crest hydrothermal activity and the balances of the major and minor elements in the ocean: the Galapagos data. *Earth Planet. Sci. Lett.* **46**, 1–18.

Eisenhauer A., Nägler T., Stille P., Kramers J., Gussone N., Bock B., Fietzke J., Hippler D. and Schmitt A.-D. (2004) Proposal for an international agreement on Ca notation as a result of the discussion from the workshop on stable isotope measurements in Davos (Goldschmidt 2002) and Nice (EGS-AGU-EUG 2003). *Geostandards Geoanal. Res.* **28**, 149–151.

Falkowski P. G., Katz M. E., Knoll A. H., Quigg A., Raven J. A., Schofield O. and Taylor F. J. R. (2004) The evolution of modern Eukaryotic Phytoplankton. *Science* **305**, 354–360.

Fantle M. S. and DePaolo D. J. (2005) Variations in marine Ca cycle over the past 20 million years. *Earth Planet. Sci. Lett.* **237**, 102–117.

Fantle M. S. and DePaolo D. J. (2007) Ca isotopes in carbonate sediment and pore fluid from ODP Site 807 Å: the Ca^{2+}(aq)-calcite equilibrium fractionation factor and calcite recrystallization rates in Pleistocene sediments. *Geochim. Cosmochim. Acta* **71**, 2524–2546.

Farkaš J., Buhl D., Blenkinsop J. and Veizer J. (2007) Evolution of the oceanic calcium cycle during the late Mesozoic: evidence from $\delta^{44/40}$Ca of marine skeletal carbonates. *Earth Planet. Sci. Lett.* **253**, 96–111.

Garrels R. M. and Mackenzie F. T. (1971) *Evolution of Sedimentary Rocks*. W.W. Norton and Company, New York, 397 pp..

Gradstein F. M., Ogg J. G., Ogg J. G., Smith A. G., Agterberg F. P., Bleeker W., Cooper R. A., Davydov V., Gibbard P., Hinnov L., House M. R., Lourens L., Luterbacher H.-P., McArthur J., Melchin M. J., Robb L. J., Shergold J., Villeneuve M., Wardlaw B. R., Ali J., Brinkhuis H., Hilgen F. J., Hooker J., Howarth R. J., Knoll A. H., Laskar J., Monechi S., Powell J., Plumb K. A., Raffi I., Röhl U., Sanfilippo A., Schmitz B., Shackleton N. J., Shields G. A., Strauss H., Van Dam J., Veizer J., van Kolfschoten Th. and Wilson D. (2004) *A Geologic Time Scale*. Cambridge University Press, Cambridge.

Gussone N., Eisenhauer A., Heuser A., Dietzel M., Bock B., Böhm F., Spero H. J., Lea D. W., Bijma J. and Nägler T. (2003) Model for kinetic effects on calcium isotope fractionation (δ^{44}Ca) in inorganic and cultured planktonic foraminifera. *Geochim. Cosmochim. Acta* **67**, 1375–1382.

Gussone N., Eisenhauer A., Tiedemann R., Haug G. H., Heuser A., Bock B., Nägler T. and Müller A. (2004) Reconstruction of Caribbean sea surface temperature and salinity fluctuations in response to the Pliocene closure of the Central American gateway and radiative forcing, using $\delta^{44/40}$Ca, δ^{18}O and Mg/Ca ratios. *Earth Planet. Sci. Lett.* **227**, 201–214.

Gussone N., Böhm F., Eisenhauer A., Dietzel M., Heuser A., Teichert B. M. A., Reitner J., Wörheide G. and Dullo W.-Ch. (2005) Calcium isotope fractionation in calcite and aragonite. *Geochim. Cosmochim. Acta* **69**, 4485–4494.

Gussone N., Langer G., Thoms S., Nehrke G., Eisenhauer A., Riebesell U. and Wefer G. (2006) Cellular calcium pathways and isotope fractionation in Emiliania huxleyi. *Geology* **34**, 625–628.

Hansen K. W. and Wallmann K. (2003) Cretaceous and Cenozoic evolution of seawater composition, atmospheric O_2 and CO_2: a model perspective. *Am. J. Sci.* **303**, 94–148.

Haq B. U. and Al-Qahtani A. M. (2005) Phanerozoic cycles of sea-level change on the Arabian Platform. *GeoArabia* **10**, 127–160.

Haq B. U., Hardenbol J. and Vail P. R. (1987) Chronology of fluctuating sea-levels since the Triassic. *Science* **235**, 1156–1167.

Hardie L. A. (1996) Secular variations in seawater chemistry: an explanation for the coupled secular variation in the mineralogies of marine limestones and potash evaporites over the past 600 My. *Geology* **24**, 279–283.

Harland W. B., Armstrong R. L., Cox A. V., Craig L. E., Smith A. G. and Smith D. G. (1990) *A Geologic Time Scale*. Cambridge University Press, Cambridge.

Hensley T. M. (2006) Calcium isotope variation in marine evaporites and carbonates: applications to Late Miocene Mediterranean brine chemistry and Late Cenozoic calcium cycling in the oceans, Doctoral dissertation. University of Californian, San Diego.

Heuser A., Eisenhauer A., Böhm F., Wallmann K., Gussone N., Pearson P. N., Nägler T. F. and Dullo W.-Ch. (2005) Calcium isotope ($\delta^{44/40}$Ca) variations of Neogene planktonic foraminifera. *Paleoceanography* **20**, PA2013. doi:10.1029/2004PA001048.

Heuser A., Eisenhauer A., Gussone N., Bock B., Hansen B. T. and Nägler T. F. (2002) Measurement of calcium isotopes ($\delta^{44/40}$Ca) using a multicollector TIMS technique. *Int. J. Mass Spectrom.* **220**, 387–399.

Hippler D., Gussone N., Darling K., Eisenhauer A. and Nägler T. (2002) δ^{44}Ca in N. pachy (left): a new SST-proxy in polar regions. *Geochim. Cosmochim. Acta* **66**(Suppl. 1), A331.

Hippler D., Schmitt A.-D., Gussone N., Heuser A., Stille P., Eisenhauer A. and Nägler T. (2003) Ca isotopic composition of various standards and seawater. *Geostandards Newsl.* **27**, 13–19.

Hippler D., Villa I., Nägler Th. F. and Kramers J. (2004) A ghost haunts mass spectrometry: real isotope fractionation or analytical paradox? *Geochim. Cosmochim. Acta* **68/11**(Suppl. 1), A215.

Holland H. D. (2005) Sea level, sediments and the composition of seawater. *Am. J. Sci.* **305**, 220–239.

Holland H. D. and Zimmermann H. (2000) The dolomite problem revisited. *Int. Geol. Rev.* **42**, 481–490.

Horita J., Zimmermann H. and Holland H. D. (2002) Chemical evolution of seawater during the Phanerozoic: implications from the record of marine evaporites. *Geochim. Cosmochim. Acta* **66**, 3733–3756.

Immenhauser A., Nägler T., Steuber T. and Hippler D. (2005) A critical assessment of mollusk $^{18}O/^{16}O$, Mg/Ca, and $^{44}Ca/^{40}Ca$ ratios as proxies for Cretaceous seawater temperature seasonality. *Palaeogeogr. Palaeoclimatol. Palaeoecol.* **215**, 221–237.

Jeppsson L., Eriksson M. E. and Calner M. (2006) A latest Llandovery to latest Ludlow high-resolution biostratigraphy based on the Silurian of Gotland—a summary. *GFF* **128**, 109–114.

Kampschulte A. and Strauss H. (2004) The sulfur isotopic evolution of Phanerozoic seawater based on the analysis of structurally substituted sulfate in carbonates. *Chem. Geol.* **204**, 255–286.

Kasemann S. A., Hawkesworth Ch. J., Pravec A. R., Fallick P. N. and Pearson P. N. (2005) Boron and calcium isotope composition in Neoproterozoic carbonate rocks from Namibia: evidence for extreme environmental change. *Earth Planet. Sci. Lett.* **231**, 73–86.

Kiessling W. (2002) Secular variations in the Phanerozoic reef ecosystem. In: *Phanerozoic Reef Patterns* (eds. W. Kiessling and J. Golonka). Soc. Econ. Paleontologists Mineralogists Spec. Pub. No. 72, Tulsa, Okla, pp. 625–690.

Kreissig K. and Elliott T. (2005) Ca isotope fingerprints of early crust-mantle evolution. *Geochim. Cosmochim. Acta* **69**, 165–176.

Langer G. (2005) Calcification of selected coccolithophore species: strontium partitioning, calcium isotope fractionation and dependence on seawater carbonate chemistry. Ph.D. thesis, University of Bremen, 169 pp.

Lemarchand D., Wasserburg G. J. and Papanastassiou D. A. (2004) Rate-controlled calcium isotope fractionation in synthetic calcite. *Geochim. Cosmochim. Acta* **68**, 4665–4678.

Locklair R. E. and Lerman A. (2005) A model of the Phanerozoic cycles of carbon and calcium in the global ocean: evaluation and constraints on ocean chemistry and input fluxes. *Chem. Geol.* **217**, 113–126.

Lowenstein T. K., Hardie M. N., Timofeeff R. V. and Demicco R. V. (2003) Secular variations in seawater chemistry and the origin of calcium chloride basinal brines. *Geology* **31**, 857–860.

Lowenstein T. K., Timofeeff R. V., Brennan S. T., Hardie M. N. and Demicco R. V. (2001) Oscillations in Phanerozoic seawater chemistry: evidence from fluid inclusions. *Science* **294**, 1086–1088.

Melim L. A., Westphal H., Swart P. K., Eberli G. P. and Munnecke A. (2002) Questioning carbonate diagenetic paradigms: evidence from the Neogene of the Bahamas. *Mar. Geol.* **185**, 27–53.

Morse J. W., Wang Q. and Tsio M. Y. (1997) Influences of temperature and Mg:Ca ratio on $CaCO_3$ precipitates from seawater. *Geology* **25**, 85–87.

Munnecke A. and Westphal H. (2005) Variations in primary aragonite, calcite, and clay in fine-grained calcareous rhythmites of Cambrian to Jurassic age—an environmental archive? *Facies* **51**, 611–626.

Nelson D. R. and McCulloch M. T. (1989) Petrogenetic applications of the ^{40}K–^{40}Ca radiogenic decay scheme—a reconnaissance study. *Chem. Geol.* **79**, 275–293.

Nägler T., Eisenhauer A., Müller A., Hemleben C. and Kramers J. (2000) The $\delta^{44}Ca$-temperature calibration on fossil and cultured Globigerinoides sacculifer: new tool for reconstruction of past sea surface temperatures. *Geochem. Geophys. Geosyst.* **1**. doi:10.1029/2000GC000091.

Ries J. B. (2004) Effect of ambient Mg/Ca ratio on Mg fractionation in calcareous marine invertebrates: a record of the oceanic Mg/Ca ratio over the Phanerozoic. *Geology* **32**, 981–984.

Russell W. A., Papanastassiou D. A. and Tomberllo T. A. (1978) Ca isotope fractionation on the Earth and other solar system materials. *Geochim. Cosmochim. Acta* **42**, 1075–1090.

Samtleben C., Munnecke A. and Bickert T. (2000) Development of facies and C/O-isotopes in transects through the Ludlow of Gotland: evidence for global and local influences on a shallow-marine environment. *Facies* **43**, 1–38.

Samtleben C., Munnecke A., Bickert T. and Pätzold J. (2001) Shell succession, assemblage and species dependent effects on the C/O-isotope composition of brachiopods—examples from the Silurian of Gotland. *Chem. Geol.* **175**, 61–107.

Sandberg P. A. (1975) New interpretations of Great Salt Lake ooids and of ancient nonskeletal carbonates mineralogy. *Sedimentology* **22**, 497–537.

Sandberg P. A. (1983) An oscillating trend in Phanerozoic nonskeletal carbonate mineralogy. *Nature* **305**, 19–22.

Schmitt A.-D., Bracke G., Stille P. and Kiefel B. (2001) The calcium isotope composition of modern seawater determined by Thermal Ionization Mass Spectrometry. *Geostand. Newsl.* **25**, 267–275.

Schmitt A.-D., Stille P. and Vennemann T. (2003a) Variations of the $^{44}Ca/^{40}Ca$ ratio in seawater during the past 24 million years: evidence from $\delta^{44}Ca$ and $\delta^{18}O$ values of Miocene phosphates. *Geochim. Cosmochim. Acta* **67**, 2607–2614.

Schmitt A.-D., Chabaux F. and Stille P. (2003b) The calcium riverine and hydrothermal isotopic fluxes and the oceanic calcium mass balance. *Earth Planet. Sci. Lett.* **213**, 503–518.

Scotese C. R. (1997) Paleogeographic Atlas, PALEOMAP Progress Report 90-0497. Department of Geology, University of Texas at Arlington, Arlington, TX, 37 pp.

Scotese C. R., MacKinnon D. I., Marlatt J. R., Reilly W. J., Smith A. G. and Stanford B. D. (1994) Continental Drift, sixth ed., The PALEOMAP Project.

Skulan J. L., DePaolo D. J. and Owens T. L. (1997) Biological control of calcium isotopic abundances in the global calcium cycle. *Geochim. Cosmochim. Acta* **61**, 2505–2510.

Soudry D., Segal I., Nathan Y., Glenn C. R., Halicz L., Lewy Z. and VonderHaar D. L. (2004) $^{44}Ca/^{42}Ca$ and $^{143}Nd/^{144}Nd$ isotope variations in Cretaceous-Eocene Tethyan francolites and their bearings on phosphogenesis in the southern Tethys. *Geology* **32**, 389–392.

Soudry D., Glenn C. R., Nathan Y., Segal I. and VonderHaar D. L. (2006) Evolution of Tethyan phosphogenesis along the northern edges of the Arabian-African shield during the Cretaceous-Eocene as deduced from temporal variations of Ca and Nd isotopes and rates of P accumulation. *Earth Sci. Rev.* **78**, 27–57.

Spencer R. J. and Hardie L. A. (1990) Control of seawater composition by mixing of river waters and mid-ocean ridge hydrothermal brines. In: *Fluid–Mineral Interactions: A Tribute to H.P. Eugster* (eds. R. J. Spencer and I.-M. Chou), Special Publication 2. Geochemical Society, pp. 409–419.

Stanley S. M. and Hardie L. A. (1998) Secular oscillations in the carbonate mineralogy of reef-building and sediment-producing organisms driven by tectonically forced shifts in seawater chemistry. *Palaeogeogr. Palaeoclimatol. Palaeoecol.* **144**, 3–19.

Steuber T. and Buhl D. (2006) Calcium-isotope fractionation in selected modern and ancient marine carbonates. *Geochim. Cosmochim. Acta* **70**, 5507–5521.

Steuber T. and Rauch M. (2005) Evolution of the Mg/Ca ratio of Cretaceous seawater: implications from the composition of biological low-Mg calcite. *Mar. Geol.* **217**, 199–213.

Steuber T. and Veizer J. (2002) Phanerozoic record of plate tectonic control of seawater chemistry and carbonate sedimentation. *Geology* **30**, 1123–1126.

Tipper E. T., Galy A. and Bickle M. J. (2006) Riverine evidence for a fractionated reservoir of Ca and Mg on the continents: implications for the oceanic Ca cycle. *Earth Planet. Sci. Lett.* **247**, 267–279.

Tomašových A. (2004) Postmortem durability and population dynamics affecting the fidelity of brachiopod size-frequency distributions. *Palaios* **19**, 477–496.

Tyrrell T. and Zeebe R. E. (2004) History of carbonate ion concentration over the last 100 million years. *Geochim. Cosmochim. Acta* **68**, 3521–3530.

Vail P. R., Mitchum R. M., Jr. and Thompson S., III. (1977) Global cycles of relative changes of sea level. In *Seismic Stratigraphy and Global Changes of Sea Level* (ed. C. E. Payton), Memoir 26, American Association of Petroleum Geologists pp. 83–97.

van Geldern R., Joachimski M. M., Daly J., Jansen U., Alvarez F., Yolkin E. A. and Ma X.-P. (2006) Carbon, oxygen and strontium isotope records of Devonian brachiopod shell calcite. *Palaeogeogr. Palaeoclimatol. Palaeoecol.* **240**, 47–67.

Veizer J. (1983) Chemical diagenesis of carbonates: theory and application of trace element technique. In *Stable Isotopes in Sedimentary Geology: Society of Economic Paleontologists and Mineralogists* (eds. M. A. Arthur, T. F. Anderson, I. R. Kaplan, J. Veizer and L. Land), Short Course, vol. 10, 1983, pp. III/1–III/100.

Veizer J., Ala D., Azmy K., Bruckschen P., Buhl D., Bruhn F., Carden G. A. F., Diener A., Ebneth S., Godderis Y., Jasper T., Korte Ch., Pawellek F., Podlaha O. and Strauss H. (1999) $^{87}Sr/^{86}Sr$, $\delta^{13}C$ and $\delta^{18}O$ evolution of Phanerozoic seawater. *Chem. Geol.* **161**, 59–88.

Veizer J. and Mackenzie F. T. (2003) The chemical composition of ancient ocean. In: *Evolution of Sedimentary Rocks* (eds. F. T. Mackenzie, H. D. Holland and K. K. Turkenian), vol. 7, Treatise on Geochemistry Elsevier-Pergamon, Oxford, pp. 369–407.

Voigt S., Gale A. S. and Flögel S. (2004) Midlatitude shelf seas in the Cenomanian–Turonian greenhouse world: temperature evolution and North Atlantic circulation. *Paleoceanography* **19**, PA4020. doi:10.1029/2004PA001015.

Wallmann K. (2001) Controls on the Cretaceous and Cenozoic evolution of seawater composition, atmospheric CO_2 and climate. *Geochim. Cosmochim. Acta* **65**, 3005–3025.

Wallmann K. (2004) Impact of atmospheric CO_2 and galactic cosmic radiation on Phanerozoic climate change and the marine $\delta^{18}O$ record. *Geochem. Geophys. Geosyst.* **5**, Q06004. doi:10.1029/2003GC000683.

Wiegand B. A., Chadwick O. A., Vitousek P. M. and Wooden J. L. (2005) Ca cycling and isotopic fluxes in forested ecosystems in Hawaii. *Geophys. Res. Lett.* **32**, L11404. doi:10.1029/2005GL022746.

Yang W., DePaolo D., Ingram L. and Owens T. (2006) Stable Ca, H and O isotopes in the modern death valley hydrological system, California. *EOS Trans. AGU*, **87**, Fall Meet. Suppl., Abstract H11I-07.

Zhu P. and Macdougall J. D. (1998) Calcium isotopes in the marine environment and the oceanic calcium cycle. *Geochim. Cosmochim. Acta* **62**, 1691–1698.

Zimmermann H. (2000) Tertiary seawater chemistry-implications from fluid inclusions in primary marine halite. *Am. J. Sci.* **300**, 723–767.

Associate editor: Juske Horita